UNIVERSITA' DEGLI STUDI DI PARMA
Dottorato di Ricerca in Fisiopatologia Sistemica
XXVIII° ciclo

Modulation of Sarco/Endoplasmic Reticulum Ca^{2+}-ATPase 2 (SERCA2) function by acetylation following the treatment with histone deacetylase inhibitor suberoylanilide hydroxamic acid (SAHA)

Coordinatore:
Chiar.mo Prof. Enrico Maria Silini

Tutore:
Chiar.ma Prof.ssa Donatella Stilli

Co-tutore:
Dott.ssa Alessandra Rossini

Dottoranda:
Maria Cristina Florio

I dati ed i metodi di ricerca originali descritti in questo elaborato sono coperti da embargo fino al 1° giugno 2018 in quanto facenti parte di un progetto di ricerca/studio più ampio avviato da Accademia Europea di Bolzano, conformemente a quanto previsto dalle linee guida fornite dall'Università di Parma.

Data and research methods described in this thesis are part wider research project of European Academy of Bolzano, so are protected by embargo until June 1st 2018, in accordance with the guidelines provided by the University of Parma.

L'uso delle illustrazioni e delle tabelle contenute nelle sezioni Introduzione e Metodi di questo elaborato è stato debitamente richiesto e autorizzato dall'avente titolo, riportato in citazione e referenza.

Permissions to use figures and table shown in the Introduction and Methods sections of this thesis has been required and obtained from the rights holder of the material.

Life is like sailing.

You can use any wind to go in any direction.

- Robert Brault –

CONTENTS

ACKNOWLEDGEMENTS

I would like to express my gratitude to all the persons who shared with me this experience and helped me to make it possible:

Dr. Alessandra Rossini and Prof. Donatella Stilli for supervising the project, for the precious scientific contribution and for continuous support of my scientific development.

Dr. Chiara Piubelli for the enthusiastic scientific support, productive discussion, and friendly

Dr. Francisco Domingues and Dr. Christian Weichenberger for the scientific and technical contribution in the context of bioinformatic analysis.

Dr. Leonardo Bocchi and Dr. Monia Savi, who introduce me to experiments with rats (a special thanks also to rats and zebrafish, without their contribution this project would not be possible).

Dr. Corrado Corti and Dr. Silvia Suffredini for brilliant help in molecular biology and electrophysiology, respectively.

All laboratory people, from Milano to Bolzano, especially Viviana for the precious constant friendship.

My family for having always supported me and believed in me.

All my friends: Daniela and Ilaria, Andre and Vero (*plus* Giulia), Adri, Alice and Fulvio, and Vale, Laura and Emilio (*plus* Lidia), and of course Michele for being irrefutable, overwhelmingly landmarks in my life. Without you, life would not be so interesting, inspiring, and exciting.

ABBREVIATION LIST

A = Arginine
AP = Action Potential
ATP = Adenosine TriPhosphate
BSA = Bovine Serum Albumin
Ca^{2+} = Calcium
CICR = Calcium Induced Calcium Release
CM = Cardiomyocyte
DMSO = Dimethyl sulfoxide
DNA = Deoxyribonucleic acid
HAT = Histone AcetylTransferase
HDAC = Histone DeAcetylase
HEK = Human Embryonic Kidney 293 cells
HEK-MSR1 = Human Embryonic Kidney 293 cells with Macrophage Scavenger Receptor 1
K = Lysine
kDa = kiloDalton
Na^{+} = Sodium
NAD^{+} = oxidized Nicotinamide adenine dinucleotide
NADH = reduced Nicotinamide adenine dinucleotide
NCX = Na^{+} - Ca^{2+} exchanger
PBS = Phosphate Buffered Saline
PCR = Polymerase Chain Reaction
PLB = Phosholamban
PTM = Post-Translational Modifications
Q = Glutamine
RNA = Ribonucleic acid
RyR = Ryanodine Receptor
SAHA = Suberoylanilide Hydroxamic Acid
SDS – PAGE = Sodium Dodecyl Sulphate - PolyAcrylamide Gel Electrophoresis
SERCA = Sarco (Endo) Plasmic Reticulum Ca^{2+} ATPase
SLN = Sarcolipin
SR = Sarcoplasmic Reticulum
SUMO = Small Ubiquitin-like Modifier
SUMOylation = Small Ubiquitin-like Modifier conjugation

ABSTRACT

Background: Acetylation and deacetylation at specific lysine (K) residues is mediated by histone acetylases (HATs) and deacetylases (HDACs), respectively. HATs and HDACs act on both histone and non-histone proteins, regulating various processes, including cardiac impulse propagation. Aim of the present work was to establish whether the function of the Ca^{2+} ATPase SERCA2, one of the major players in Ca^{2+} reuptake during excitation-contraction coupling in cardiac myocytes (CMs), could be modulated by direct K acetylation.

Materials and methods: HL-1 atrial mouse cells (donated by Prof. Claycomb), zebrafish and Streptozotocin-induced diabetic rat CMs were treated with the pan-inhibitor of class I and II HDACs suberanilohydroxamic acid (SAHA) for 1.5 hour. Evaluation of SERCA2 acetylation was analyzed by co-immunoprecipitation. SERCA2 activity was measured on microsomes by pyruvate/NADH coupled reaction assay. SERCA2 mutants were obtained after cloning wild-type and mutated sequences into the pCDNA3 vector and transfected into HEK cells. Ca^{2+} transients in CMs (loading with Fluo3-AM, field stimulation, 0.5 Hz) and in transfected HEK cells (loading with FLUO-4, caffeine pulse) were recorded.

Results: Co-Immunoprecipitation experiments performed on HL-1 cells demonstrated a significant increase in the acetylation of SERCA2 after SAHA-treatment (2.5 μM, n=3). This was associated with an increase in SERCA2 activity in microsomes obtained from HL-1 cells, after SAHA exposure (n=5). Accordingly, SAHA-treatment significantly shortened the Ca^{2+} reuptake time of adult zebrafish CMs. Further, SAHA 2.5 nM restored to control values the recovery time of Ca^{2+} transients decay in diabetic rat CMs. HDAC inhibition also improved contraction parameters, such as fraction of shortening, and increased pump activity in microsomes isolated from diabetic CMs (n=4). Notably, the K464, identified by bioinformatic tools as the most probable acetylation site on human SERCA2a, was mutated into Glutamine (Q) or Arginine (R) mimicking acetylation and deacetylation respectively. Measurements of Ca^{2+} transients in HEK cells revealed that the substitution of K464 with R significantly delayed the transient recovery time, thus indicating that deacetylation has a negative impact on SERCA2 function.

Conclusions: Our results indicate that SERCA2 function can be improved by pro-acetylation interventions and that this mechanism of regulation is conserved among

species. Therefore, the present work provides the basis to open the search for novel pharmacological tools able to specifically improve SERCA2 activity in diseases where its expression and/or function is impaired, such as diabetic cardiomyopathy.

INTRODUCTION

SERCA PUMP

The Sarco(Endo)plasmic Reticulum (SR) Ca^{2+} ATPase (SERCA) is a calcium pump that translocates two Ca^{2+} ions from the cytosol into the SR lumen by using energy of ATP hydrolysis. SERCA is a single polypeptide with a molecular weight of approximately 110 kDa and organized into four different domains [1]:

- a transmembrane domain with ten transmembrane helices
- a nucleotide (ATP) binding site
- a phosphorylation/catalytic domain that drives ATP hydrolysis
- an actuator domain that catalyzes dephosphorylation of the phosphorylation domain.

SERCA is a P-type ATPase transporter, characterized by the reversible conformational change secondary to the reversible transfer of the terminal phosphate from ATP to the protein catalytic domain [2, 3]. Three different SERCA genes have been identified so far in vertebrates [4], showing high degree of conservation among species [5]: *ATP2A*, *ATP2A2* and *ATP2A3*, encoding for the SERCA1, SERCA2 and SERCA3 proteins, respectively. Due to alternate splicing mechanisms, different protein isoforms are produced, whose expression is regulated in a tissue specific manner and during development [4]. SERCA1 isoforms are expressed in fast skeletal muscle. SERCA2 can have different isoforms (Figure 1): SERCA2a is expressed in heart and slow muscles, while SERCA2b is expressed ubiquitously. SERCA3 is encoded by the third gene and is reported to be expressed in non-muscle cells [6].
SERCA2a has been described as the most expressed in cardiac muscle [4, 6] and SERCA2b has been found in cardiomyocytes, but at a lower extent [4] and with different SR compartmentalization compared to the 2a isoform [7].

Recently, SERCA2c (a less conserved isoform, restricted to humans) has been also described in epithelial cells [8] and in a confined area of cardiomyocytes, very near to the sarcolemma [9,10].

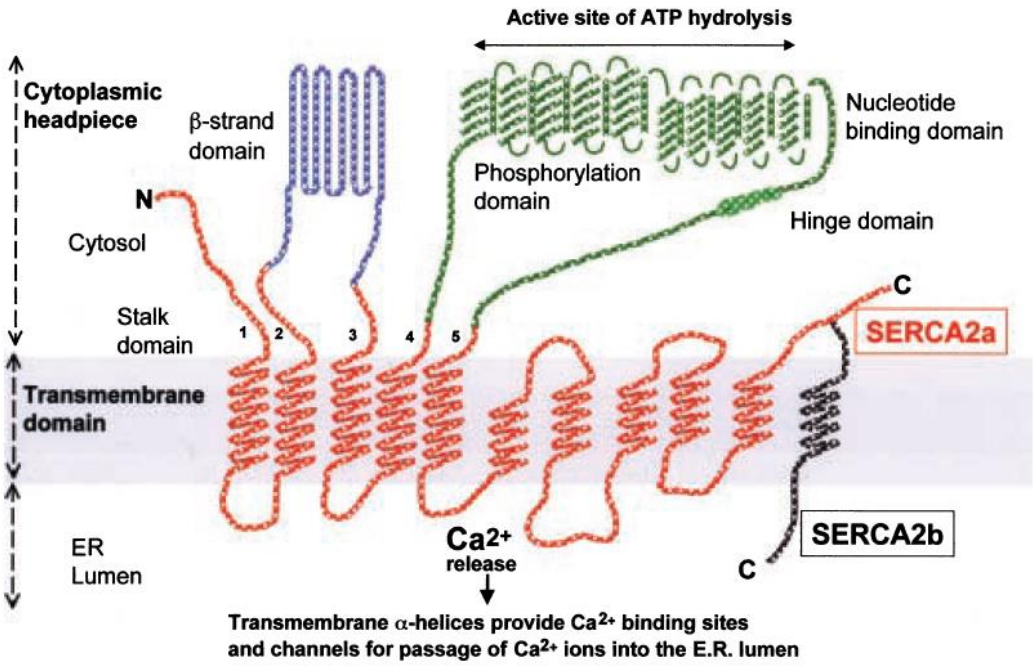

Figure 1: Predicted secondary structure of SERCA2. The molecule is anchored to the membrane of sarcoplasmic reticulum by 10 helices; both the N- and C-terminal segments of SERCA2a are exposed in the cytoplasm, while SERCA2b has a longer tail section into the lumen of reticulum. In the phosphorylation and nucleotide binding domains the active site necessary for ATP hydrolysis is formed. The transmembrane domain contains Ca^{2+} binding sites and it forms the channel for transport of Ca^{2+} into the SR (from Dhitavat J. et al, British Journal of Dermatology, 2004 [11]).

SERCA2 plays a pivotal role for the level of SR Ca^{2+} load and for the majority of the cytosolic calcium removal (70% in human, 92% in mouse and rat [12]) generating the cardiac diastolic phase, thus representing a key player for cardiomyocytes contraction and relaxation [13]. Modifications of Ca^{2+} dynamic associated with reduced SERCA2 expression and function have been described in hypertrophic [14], failing [15], and dilated hearts [16]. Of note, variations in SERCA2 are documented among the major factors that cause the diastolic dysfunction observed in diabetic cardiomyopathy [17, 18].

CARDIAC CALCIUM HANDLING

Cardiac excitation-contraction coupling (ECC) is the process whereby an action potential triggers a myocyte to contract. Calcium ion is the second messenger crucial in cardiac electrical activity and it is the most important responsible for the activation of the myofilaments, able to cause contraction [13].

When the cardiac action potential arrives, Ca^{2+} enters into the cell through sarcolemmal L-type Ca^{2+} channels activated by depolarization and produces an inward Ca^{2+} current (I_{Ca}), which contributes to the plateau phase of action potential (Figure 2). The entry of a small quantity of calcium through the L-type Ca^{2+} channel ("trigger") produces a localized increase of intracellular Ca^{2+} concentration in the space among the surface and SR membranes [19, 20]. The slight increase in intracellular Ca^{2+} concentration induces the release of calcium ions from the sarcoplasmic reticulum, through a specific release channels, the ryanodine receptors (RyRs). This mechanism is defined as CICR, Ca^{2+}-induced Ca^{2+} release. The rise of intracellular calcium concentration increases the open probability of the RyRs, resulting in the release of calcium ions into the cytoplasm from the SR.

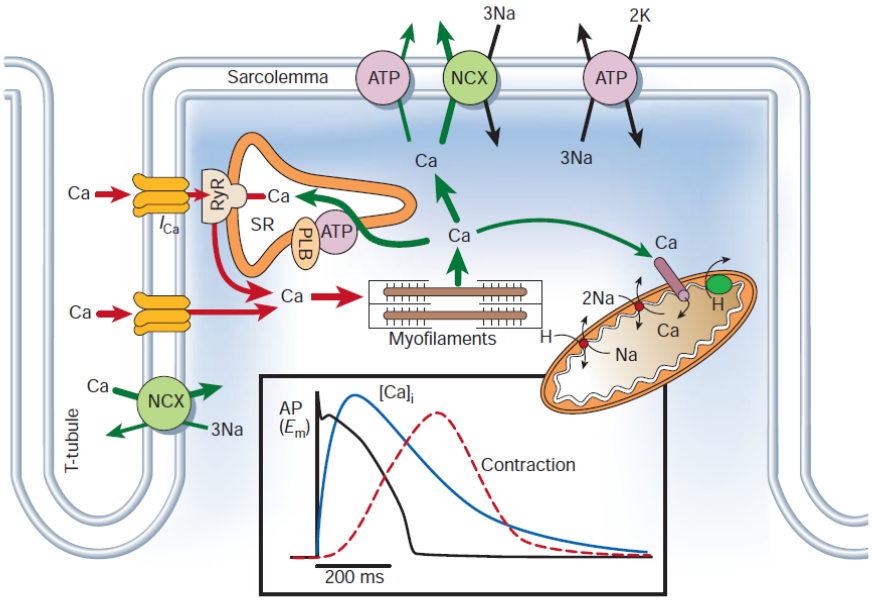

Figure 2: Scheme of Ca^{2+} transport in ventricular myocytes. In the insertion there is described the time course of an action potential, Ca^{2+} transient and contraction measured in a rabbit ventricular myocyte. Abbreviations: NCX, Na^{+}/Ca^{2+} exchanger; ATP, ATPase; PLB, phospholamban; SR, Sarcoplasmic Reticulum (modified by Bers D.M., Nature, 2002 [13]).

The combination of Ca^{2+} entry and release raises the free cytoplasmatic Ca^{2+} concentration ($[Ca^{2+}]_i$), allowing the binding between calcium and myofilament protein troponin C, which is the first player for the contractile machinery. In order to start the relaxation phase, $[Ca^{2+}]_i$ must decline, with the consequent Ca^{2+} dissociation from troponin.

Hence, relaxation is induced by a reduction of $[Ca^{2+}]_i$ made by different mechanisms:

SR Ca^{2+}-ATPase, that reuptakes calcium into the SR, sarcolemmal Sodium-Calcium exchanger (NCX) and sarcolemmal Ca^{2+}-ATPase, that extrude calcium outside the cell, and mitochondrial Ca^{2+} uniporter, that brings calcium into mitochondria. SERCA2 and NCX are most important quantitatively, even though the quantitative involvement can differ among different species [13, 21].

For example, in rabbit ventricular myocytes, SERCA2 removes 70% of the activator calcium, NCX removes 28%, and the left 1% is removed by the sarcolemmal Ca^{2+}-ATPase and mitochondrial Ca^{2+} uniporter (also known as “the slow systems” [13]). In rat ventricular myocytes the activity of SERCA2 is higher, due to a major concentration

of pump molecules [22], and NCX involvement is lower, resulting in a balance of 92% for SERCA2, 7% for NCX and 1% for the slow systems (Figure 3). Analysis in mouse ventricle is quantitatively similar to rat [23], whereas dog, cat, guinea-pig and human ventricles are more like rabbit [13]. Interestingly, in heart failure in humans and rabbits, expression and function of calcium ATPase are reduced and extrusion via NCX is increased [24], therefore these components give a more similar contribution to the decrease of intracellular calcium concentration. These changes tend to reduce calcium content in the SR, thus limiting Ca^{2+} release and causing systolic contractile dysfunction in heart failure [25].

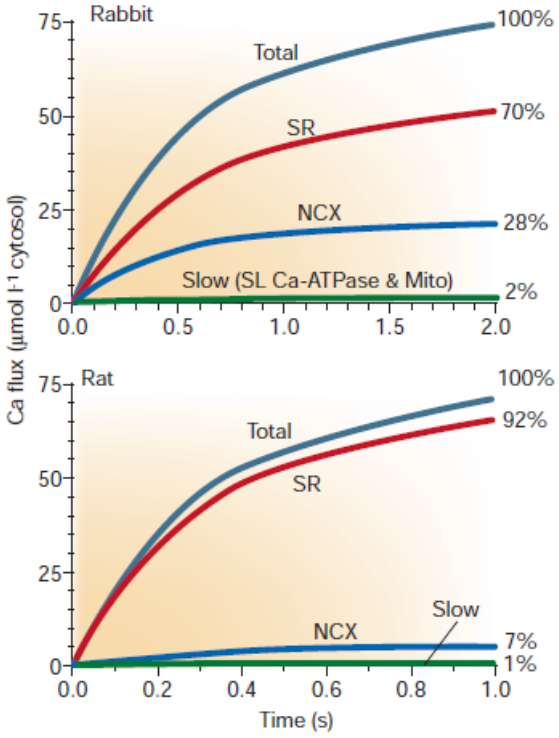

Figure 3: Different quantitative Ca^{2+} fluxes during excitation–contraction coupling. Ca^{2+} fluxes measured in rabbit (upper panel) and rat (lower panel) ventricular myocytes during relaxation. Curves consider $[Ca^{2+}]_i$ and $[Ca^{2+}]_i$ dependence of transport rates for each system. Percentages are in relation to the contributions to Ca^{2+} removal. Abbreviations: NCX, Na^+/Ca^{2+} exchanger; SL, Ssarcolemmal; SR, SR Ca2+-ATPase; Mito, Mitochondrial Ca2+ uniporter (modified by Bers D.M., Nature, 2002 [13]).

REGULATION OF SERCA2

As mentioned above, Ca^{2+} is critically significant in regulation of contraction/relaxation processes, therefore the mechanism of SERCA pump has already been investigated [1]. Among the different P-type ion translocating ATPases, SERCA1a is the best characterized both on structural and functional point of view. In E1 conformational state, transmembrane Ca^{2+} binding sites have high affinity and expose to cytoplasm, while in E2 have low affinity and expose to lumen of sarcoplasmic reticulum. The effective transmission of calcium ions occurs between two phosphorylated intermediates state, E1P and E2P (panel in figure 4 describes a simplified scheme of reaction).

In 2000, rabbit SERCA1a structure was crystallized in phospholipid bilayer and its atomic structure was solved [26]. Due to the fact that SERCA1 and SERCA2 are close homologues for 83% of sequence identity, it is possible to use the structure of rabbit SERCA1, and relative structural and functional analysis [1] to understand the functional system of SERCA2. Reaction cycle consists in different states (Figure 4). As mentioned above SERCA has four different domains: the A-domain, connected to the M1–M3 helices with rather long linkers, acts as the actuator of the transmembrane passage that regulates Ca^{2+} binding and release [27, 28]; the P-domain contains several critical residues that characterize the P-type ATPase and has a wedge-shape and a flat top surface to allow a rotation of the A-domain on the top surface of the P-domain [28]; the N-domain is a long insert between two portions forming the P-domain and some important residues (e.g. for adenosine binding and binding ATP) are contained in this domain [27, 29]; the M-domain contains 10 transmembrane helices and during the reaction cycle, all helices from M1 to M6 move significantly, while helices from M7 to M10 apparently act as membrane anchors.

The E2 state is the consequent state to the release of calcium ions into the lumen. Four different major enzyme states occur during the reaction cycle, in addition to other intermediate reactions, named E1-P, E2P, E2-P*, and E1/E2, described below [30]. ATP derived energy is used to exchange 2 calcium ions from the cytoplasm into the SR with 1-3 protons into the cytoplasm and to start the reaction cycle (E1/E2 state). Consequently, the phosphorylation site between the ATP-bound N-domain and the P domain is assembled and the A-domain guides the occlusion of bound calcium ions: in this state calcium ions are hidden without any access to both side of membrane. The E1-

P state starts when a kinase reaction occurs, following the phosphorylation of P-domain with production of ADP. ATP is hydrolyzed to ADP, resulting in the phosphorylation of Asp351. The protein modifies from the E1 to the E2 conformation and the calcium ions are transported across the membrane and released into the lumen of the sarcoplasmic reticulum. Specifically, this allows the rotation of A-domain near the phosphorylation site, creating a stable association with both the P- and the N- domains. A-domain's movement applies an impulse on M3-M4 and a drag on M1-M2, driving the pump to expose at the luminal side and starting the E2P state. During this conversion, the Ca^{2+}-binding residues located in the transmembrane domain are separated, abolishing the high-affinity binding site [31, 32]. Protons and water molecules enter and stabilize the Ca^{2+}-binding sites, now empty [33]. In the meanwhile, the exposure of N-domain to the cytosol occurs, and the nucleotide-binding site is ready for ATP exchange. The A-domain drives the de-phosphorylation of P-domain, concluding the cycle with the release of the phosphate from the enzyme, which is stimulated by new bound ATP.

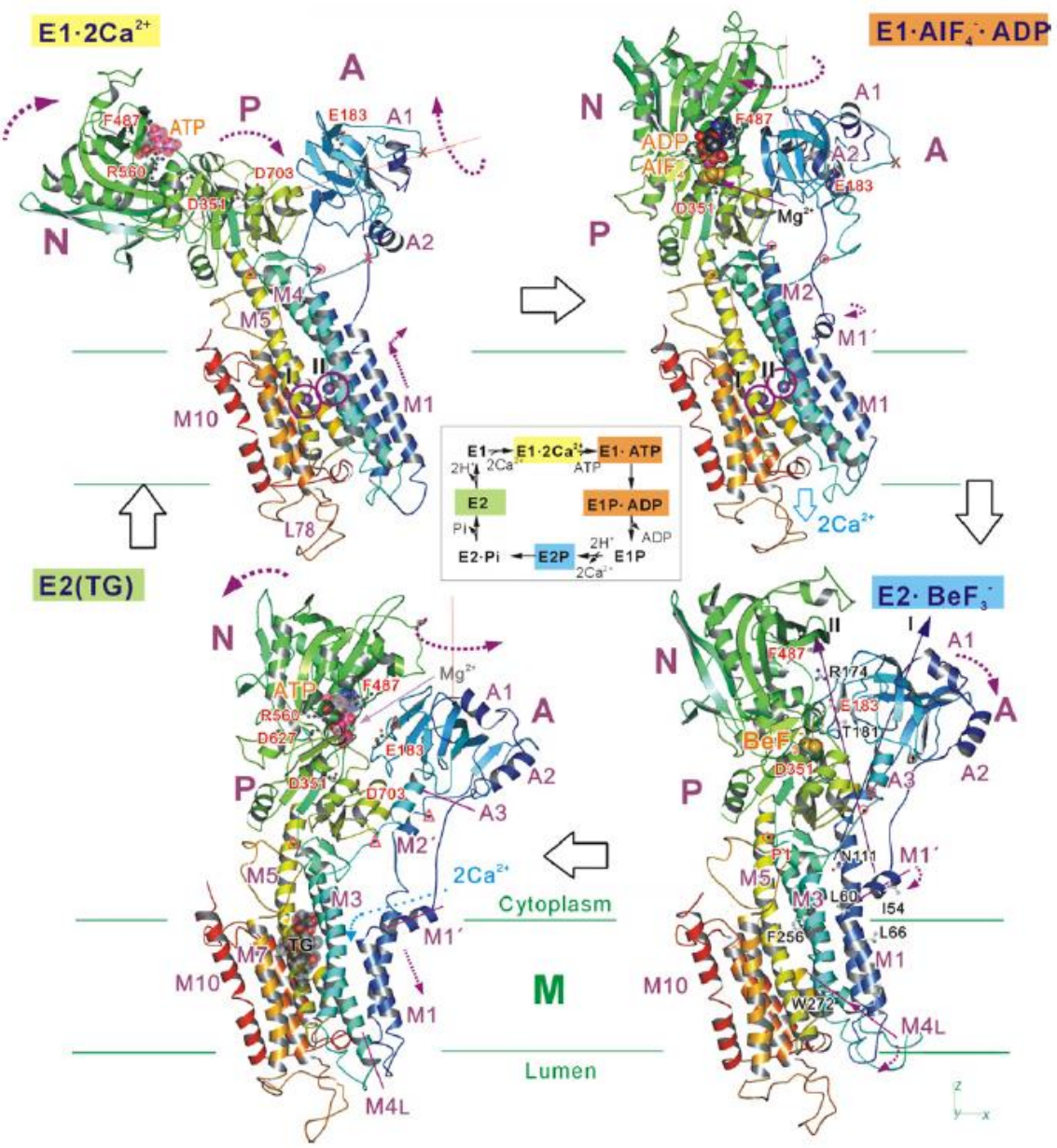

Figure 4: Different structural states of SERCA. Four different states of Ca^{2+}-ATPase and E1-E2 reaction (a simplified scheme) are described. Different colors correspond to the respective structures presented here. A, N, and P domains, and M1–M10 (helices in the transmembrane domain) are indicated (from Toyoshima C. et al, Archives of Biochemistry and Biophysics, 2008 [1]).

SERCA2a activity is controlled by two small regulatory proteins: phospholamban [34, 35, 36] and sarcolipin [37, 38, 39].

The major regulator of SERCA2 pump is phospholamban (PLB). Identified for the first time in the cardiac microsomes, it is the principal substrate for cAMP-dependant kinase (CaMKII) and the regulator of SERCA pump [40, 41, 42]. PLB is a phosphoprotein composed by 52 amino acid and its primary structure is very conserved across species. PLB is more expressed in the heart than slow twitch and smooth muscle tissues and it is one of the mediator of the β-adrenergic responses in the cardiac muscle. Moreover, phosphorylation of PLB at Ser216 and Thr217 promoted by the Protein kinase A (PKA) and CAMKII, respectively, can induce an increase of the SERCA pump activity [35, 43, 44]. SERCA2 pump is inhibited by the dephosphorylated PLB, whereas the phosphorylation removes the inhibition and provokes a substantial increase in Ca^{2+} transport (Figure 5). Thus, the regulation of SERCA pump by PLB is considered to be the primary mechanism for β-adrenergic-mediated response of the heart, as well as for enhanced Ca^{2+} transport throughout the SR [45].

The mechanism of PLB action on SERCA pump has been studied extensively. PLB is located within cardiac sarcoplasmic reticulum both as pentamers and as monomers. Monomers are strictly connected: in fact, pentamers cannot be dissociated into monomers under normal conditions except at high temperature. Thus, extreme conditions are required to disrupt the high affinity between monomers when they are in a pentameric state. When cytoplasmic concentration of Ca^{2+} is low, PLB monomer interacts with SERCA2, thus inhibiting the pump functionality by decreasing the pump affinity for Ca^{2+}. The pump is brought to a halt temporarily during diastolic phase by the reduction in cytosolic Ca^{2+} and the low affinity for Ca^{2+} until systolic Ca^{2+} reaches the level necessary to reactivate the pump [45]. In rodents, the time between diastolic and systolic phases is very short and the SERCA pump may never completely reaches a resting state. When cytosolic Ca^{2+} levels reach a certain threshold, the inhibitory action of PLB on SERCA pump is absent. This occurs when PLB phosphorylation is missing and kinases are activated. Thus, with high levels of Ca^{2+}, the physical hydrophobic and electrostatic interactions between PLB and SERCA are reduced, allowing SERCA activation (Figure 5).

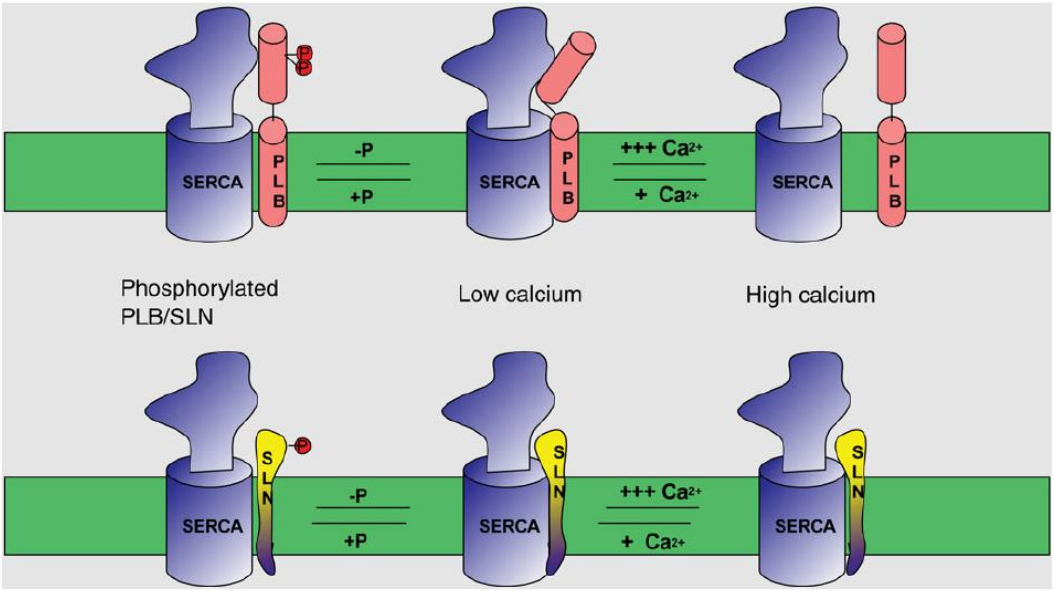

Figure 5: Theoretical model decribing SERCA pump regulation by phospholamban and sarcolipin. SERCA pump is binded by the dephosphorylated phospholamban (PLB) which regulates SERCA activity (top, middle panel). This interaction is interrupted by either phosphorylation of PLB (top, left panel) or in the presence of high calcium concentration (top, right panel). Sarcolipin (SLN) can interact with SERCA when it is unphosphorylated (bottom, middle). This interaction is more affected by phosphorylation and less affected by Ca^{2+} concentration, as described in the bottom of the figure at left and right panel, respectively (from Periasamy M. et al, Cardiovascular Research, 2008 [45]).

Sarcolipin (SLN) is a low molecular weight protein (31 amino acids), identified for the first time in co-purified preparation of skeletal muscle SERCA1a pump [37, 46, 47]. In cardiac context, SLN is more expressed in the atria than in the ventricle (Table 1) [48, 49] and its expression, in skeletal muscle tissues, changes between small and large animals [37, 50, 38], although its primary structure is very conserved across species and may suggest a comparable mechanism of regulation as for PLB. Both SLN and PLB have similar transmembrane sequences, thus indicating that they belong to the same gene family [46], but they differ at N- and C-terminus.

It has been demonstrated that SLN can inhibit SERCA pump by decreasing the calcium affinity of the pump and with a consequent effect on contractile function [47, 51, 52]. Phospholamban and sarcolipin are the major inhibitors of SERCA2a function, playing a

critical role in cardiac contractility and in mediating the β-adrenergic response, both in normal and failing hearts [37, 53].

Protein	Skeletal muscle				Cardiac muscle		Smooth muscle	Non-muscle
	Fast twitch		Slow twitch					
	Fetal	Adult	Fetal	Adult	Atria	Ventricle		
SERCA 2a	++	−	+	++	++++	+++	+	+
PLB	−	−	+	++	++	++++	++	−
SLN	+	+	++	++	++++	+	−	−

Table 1: Differential expression of SERCA2a, PLB, and SLN in rodent muscle tissues. In rodent muscle tissues differential expression of SERCA2a, PLB, and SLN occurs. SERCA2 can be detected in smooth and non-muscle cells at low levels, specifically the isoform "a" (modified from Periasamy M. et al, Cardiovascular Research, 2008 [45]).

Evidences have also been provided demonstrating that SERCA2 activity can be altered by several post-translational modifications [54]. For example, SUMOylation (Small Ubiquitin-like Modifier conjugation) [55]) and glutathionylation [56] seem to increase SERCA2 activity. On the other side, glycosylation [57] and nitration [58] are post-translational modifications able to decrease SERCA2 pump function. Moreover, Foster and coworkers [59] recently described three lysine that can be acetylated on the SERCA2 structure of guinea pig. In any case, no potential effect of SERCA2 direct acetylation has never been evaluated on intracellular Ca^{2+} dynamic.

LYSINE ACETYLATION

Acetylation of lysine is a reversible post-translational modification (PTM), that refers to the addition of an acetyl functional group on lysine residues. Specifically, acetylation plays an important role in the synthesis, stability and localization of proteins [60, 61] and plays a key role in the regulation of gene expression through the modification of core histone tails [62, 63]. In histone acetylation and deacetylation (the removal of the acetyl group), histone proteins are acetylated and deacetylated on lysine residues in the N-terminal tail as part of gene regulation through the activity of different enzymes: histone acetyltransferases or acetylases (HATs) or histone deacetylases (HDACs), that, despite their name, can modify the acetylation status of non-histone proteins as well [64, 65]. Recently, the nomenclature is being revised to lysine acetyltransferases (KATs), reflecting their ability to acetylate lysine (denoted 'K') on many proteins [66]. The KATs are various, with many assigned, based on structural similarities, to either the GNAT (Gcn5-related N-acetyltransferases) superfamily or the MYST (MOZ, YBF2/Sas3, Sas2, Tip60) family. Other important KATs include p300 (E1A-associated protein 300 kDa), CBP (cAMP response element binding - CREB - protein), and TAFII 250 (TATA-binding protein associated factor II 250). The modification of the positively charged lysine to acetyl-lysine alters protein structure and interactions with other biomolecules. For example, acetylation of histones typically stimulates the involvement of effector proteins, relaxation of chromatin status, and an improve of transcription [67].

HISTONE ACETYLASES (HATS)

HATs are traditionally divided into two different classes based on their subcellular localization [62]. Type A HATs are found in the nucleus and partecipate in the regulation of gene expression by inducing acetylation of nucleosomal histones in the context of chromatin [68]. They contain a bromodomain, which binds to acetylated lysine residues on histone substrates. Gcn5, p300/CBP, and TAFII250 are some examples of HATs of type A that cooperate with activators to enhance transcription. Type B HATs are lacking in the bromodomain and they are located in the cytoplasm and are responsible for acetylation of newly synthesized histones prior to their assembly into nucleosomes. The acetyl groups added by type B HATs to the histones are removed by HDACs once they enter into the nucleus and are incorporated into chromatin. Hat1 is one of the few known examples of a type B HAT [69]. Despite this traditional

classification, some HATs act in many complexes and/or several locations and it is not easy to fit them into a particular class [70].

HATs can be also grouped into several different families based on sequence homology as well as shared structural features and functional roles. The Gcn5-related N-acetyltransferase (GNAT) family includes Gcn5, PCAF, Hat1, Elp3, Hpa2, Hpa3, ATF-2, and Nut1. These HATs are generally characterized by the presence of a bromodomain, and they are found to acetylate lysine residues on histones H2B, H3, and H4. The MYST family of HATs is named after its four founding members MOZ, Ybf2 (Sas3), Sas2, and Tip60 [62]. These HATs are typically characterized by the presence of zinc fingers and chromodomains and they are found to acetylate lysine residues on histones H2A, H3, and H4. In addition to these HATs, there are several other proteins found normally in higher eukaryotes that exhibit HAT activity, such as p300/CBP [71]. In eukaryotes, several aspects of cellular homeostasis can be modulated by HATs and HDACs activity. For example, in yeast, the HAT Gcn5 is essential for the cell response to stress, meiosis, and DNA replication [72]. In mammals, cell growth, myotube differentiation, and apoptosis include the involvement of the HAT p300/CBP [73]. Moreover, the HAT enzyme PCAF, identified for the first time as a p300/CBP-binding protein, is recognized to play a key role in the regulation of myofilament contractile activity, the myogenic differentiation and adipocyte proliferation [74].

HISTONE DEACETYLASES (HDACS)

HDACs are classified into three main classes based on their homology to yeast proteins. HDAC1, HDAC2, HDAC3 and HDAC8 are included in class I and have homology to yeast RPD3. HDAC4, HDAC5, HDAC7 and HDAC9 belong to class IIa and are homologues to yeast HDAC1. HDAC6 and HDAC10 (included in class IIb) contain two catalytic sites, whereas HDAC11 has conserved residues in its catalytic center that are shared by both class I and class II deacetylases and it is sometimes placed in class IV [75, 76] (Table 2).

	Class I				Class IIA				Class IIB		Class IV
	HDAC1	HDAC2	HDAC3	HDAC8	HDAC4	HDAC5	HDAC7	HDAC9	HDAC6	HDAC10	HDAC11
Localization	Nucleus	Nucleus	Nucleus	Nucleus	Nucleus/cytoplasm	Nucleus/cytoplasm	Nucleus/cytoplasm	Nucleus/cytoplasm	Mostly cytoplasm	Mostly cytoplasm	Nucleus/cytoplasm
Size (amino acids)	483	488	428	377	1,084	1,122	855	1,011	1,215	669	347
Chromosomal localization	1p34.1	6q21	5q31	Xq13	2q37.2	17q21	12q13	7p21-p15	Xp11.22-23	22q13.31-q13.33	3p25.2
Catalytic sites	1	1	1	1	1	1	1	1	2	1	2
Tissue distribution	Ubiquitous	Ubiquitous	Ubiquitous	Ubiquitous/? Smooth muscle differentiation	H, SM, B	H, SM, B	H, PL, PA, SM	B, SM	H, L, K, PA	L, S, K	B, H, SM, K
Substrates (partial list)	Androgen receptor, SHP, p53, MyoD, E2F-1, Stat3	Glucocorticoid receptor, YY-1, Bcl-6, Stat3	SHP, YY-1 GATA-1, RelA, Stat3, MEF2D						α-Tubulin, Hsp90, SHP, Smad7		
Binding partners (partial list)			CDK9, SP1, PP4c	EST1B	GCMa, GATA-1, HP-1	GCMa, Smad7, HP-1	PLAG1, PLAG2		Runx2		
Knockout phenotype	EL increased histone acetylation, increase in p21 and p27	Cardiac defect			ANKRA, RFXANK	CAMPTA, REA, estrogen receptor	FOX3P, HIF-1α, Bcl-6, endothelin receptor, α-actinin 1, α-actinin 4, androgen receptor, Tip60	FOX3P			
					Defects in chondrocyte differentiation	Cardiac defect	Maintenance of vascular integrity, increase in MMP10	Cardiac defect			

Table 2: Histone deacetylases characteristics and localization. Abbreviations: H, heart; SM, skeletal muscle; B, brain; PL, placenta; PA, pancreas; L, liver; K, kidney; S, spleen; EL, embryonic lethal; Stat3, Signal transducers and activators of transcription 3; CDK9, Cyclin-Dependent Kinase 9; MMP10, Matrix metalloproteinase 10; Hsp90, Heat shock protein 90; HIF-1α, Hypoxia-Inducible Factor-α (modified from Dokmanovic M. et al, Mol Cancer Res, 2007 [77]).

The class III HDACs include sirtuins, based on their homology to yeast Sir2. They carry out the deacetylation by using nicotinamide adenine dinucleotide (NAD^+) as a cofactor instead of Zinc [78, 79].

Class I HDACs are mostly localized within the nucleus and class II HDACs are able to shuttle between nucleus and cytoplasm [80, 81] (Table 3). Up to now, more than 50 non histone proteins have been recognized as substrates for one or more HDACs [82, 83, 84]. These substrates include proteins that have regulatory roles in cell proliferation, cell migration and cell death (Table 3).

Functional Group	Protein	HDAC Implicated
Structural protein	α-Tubulin	HDAC6
Chaperone protein	Hsp90	HDAC6
DNA binding nuclear receptors	Androgen receptor	HDAC1
	Glucocorticoid receptor	HDAC2
	Estrogen receptor α	ND
	SHP	HDAC1, HDAC3, HDAC6
DNA binding transcription factors	p53	HDAC1
	p73	ND
	MEF2D	HDAC3
	GCMa	HDAC1, HDAC3, HDAC4, HDAC5
	YY1	HDAC1, HDAC2, HDAC3
	GATA-1	HDAC3, HDAC4, HDAC5
	GATA-2	HDAC3, HDAC5
	GATA-3	ND
	MyoD	HDAC1
	E2F-1	HDAC1
	E2F-2	ND
	E2F-3	ND
	RelA (in NF-κB)	HDAC3
	PLAG1, PLAG2	HDAC7
	Bcl-6	HDAC2
	c-Myc	ND
	EKLF	ND
	HIF-1α	ND
Transcription coregulators	Rb	ND
	PGC-1α	Class III
	DEK	ND
Chromatin remodeling	HMG-A1	ND
	HMG-B1	ND
	HMG-B2	ND
	HMG-N2	ND
	HMGI(Y)	ND
	SRY	HDAC3
Signaling mediators	Stat3	HDAC1, HDAC2, HDAC3
	Smad7	HDAC1, HDAC3, HDAC2, HDAC5, HDAC6
	IRS-1	ND
	β-Catenin	ND
DNA repair enzymes	Ku70	ND
	WRN	ND
Nuclear import	Importin-α7	ND

Table 3: Protein substrates of HDACs (partial list). The acetylation status of the HDAC substrates is a determinant of their structure and, as a consequence, their activity. Abbreviations: ND, not determined. HMG, High Mobility Group (modified from Dokmanovic M. et al, Mol Cancer Res, 2007 [77]).

MODULATION OF ACETYLATION / DEACETYLATION BALANCE WITH HDACS INHIBITORS

Acetylation / deacetylation balance can be modulated by different compounds able to act on HATs and HDACs activity. For example, histone deacetylase inhibitors (HDACi) have been used in psychiatry and neurology as mood stabilizers and anti-epileptics (e.g. valproic acid). Recently, HDACis are being studied for treatment for neurodegenerative diseases [85, 86] and for cancer therapy [87, 88].

HDACis are currently being investigated as chemo-sensitizers for cytotoxic chemotherapy or radiation therapy, or in association with DNA methylation inhibitors based on *in vitro* synergy [89]. HDACis act exclusively on Class I, II and Class IV HDACs by chelating zinc ions in HDAC's active site at different concentrations [90, 76]. HDACis can be divided into several structural classes including hydroxamates, cyclic peptides, aliphatic acids and benzamides [75, 83, 88] (Table 4). The first natural hydroxamate discovered to inhibit HDACs was Trichostatin-A (TSA) [91]. A series of amino suberoyl hydroxamic acids have recently been revealed to inhibit HDACs and transform cell proliferation at nanomolar concentrations [92].

Suberoylanilidehydroxamic acid (SAHA, or Vorinostat), structurally similar to TSA [93], is a pan-inhibitor of class I and class II HDAC proteins [82] and it was the first HDACi approved by the US Food and Drug Administration in October 2006 for the treatment of refractory cutaneous T-cell lymphoma (CTCL) [94].

Class	Compound	Structure	HDAC Target (Potency)	Effects on Transformed Cells	Stage of Development (Reference)
Hydroxamates	TSA		Class I and II (nmol/L)	TD; GA; A; AI; AE	N/C
	SAHA, Zolinza, vorinostat		Class I and II (μmol/L)	TD; GA; AI; AE; MF; AU; S; PP; ROS-CD	Merck Food and Drug Administration approved for CTCL (4)
	CBHA		N/A (μmol/L)	GA; A; AI; AE	Merck (4)
	LAQ-824		Class I and II (nmol/L)	GA; A; AI	Novartis phase I (discontinued)
	PDX-101		Class I and II (μmol/L)	GA; A	TopoTarget phase II (57)
	LBH-589		Class I and II (nmol/L)	GA; A; ROS-CD	Novartis phase I (51)
	ITF2357		Class I and II (nmol/L)	GA; A; AI	Italfarmaco phase I (56)
Cyclic peptide	PCI-24781 Depsipeptide (FK-228)	NA 	Class I and II (NA) Class I (nmol/L)	N/A TD; GA; A; AI; AE; MF; ROS-CD	Pharmacyclics phase I Gloucester Pharmaceuticals phase IIb for CTCL and PTCL (63) phases I and II
Aliphatic Acids	Valproic Acid		Class I and IIa (mmol/L)	TD; GA; A; S	Abbot phase II
	Phenyl butyrate		Class I and IIa (mmol/L)	TD; GA; A; AI; AE	Phase II
	Butyrate		Class I and IIa (mmol/L)	TD; GA; A; AI; AE	Phase II
	AN-9		N/A (μmol/L)	TD; GA; A	Titan Pharmaceuticals phase II
Benzamides	MS-275		HDAC1, HDAC2, HDAC3 (μmol/L)	TD; GA; A; AI; AE; ROS-CD	Schering AG phase II (51)
	MGCD0103		Class I (μmol/L)	TD; GA; A	Methylgene phase II (60)

Table 4: HDAC inhibitors (a partial list is reported). Abbreviations: GA, Growth Arrest; TD, Terminal Differentiation; A, Apoptosis; AI, cell death by activating intrinsic apoptotic pathway; AE, cell death by activating extrinsic apoptotic pathway; MF, Mitotic Failure; AU, autophagic cell death; S, Senescence; PP, polyploidy; ROS-CD, Reactive Oxygen Species-facilitated Cell Death; N/A, Not Available; CBHA, M-Carboxycinnamic acid Bishydroxamate; CTCL, Cutaneous T-Cell Lymphoma; CTCL, peripheral T-cell lymphoma (modified from Dokmanovic M. et al, Mol Cancer Res, 2007 [77]).

HDAC INHIBITION IN CARDIAC PATHO-PHYSIOLOGY

The reversible protein acetylation carried out by HATs and HDACs plays a role in the physiology of adult cardiomyocytes regulating the myofilament contractile activity. It has been demonstrated that the acetyltransferase PCAF and the class II deacetylase HDAC4 can associate with cardiac myofilaments, specifically with the Z-disc and I- and A-bands of cardiac sarcomeres. After HDAC inhibition (using class I and II HDAC inhibitors or anti-HDAC4 antibody), the acetylation of sarcomeric proteins was increased, provoking an enhancement of calcium sensitivity of myofilaments [95]. The Z-disc-associated protein, muscle LIM protein (MLP) is one of the sensor of cardiac mechanical stretch and it is identified as an acetylated target of PCAF and HDAC4.

Moreover, in a model of dystrophic mice ventricular arrhythmias are prevented and defects of conduction of the hearts are repaired after HDAC inhibition [96]. The modification in the level and/or spatial distribution of connexins is relevant for cardiac impulse transmission and plays a role in arrhythmias onset; in fact, in dystrophic mice hearts, alteration in connexin40 expression and in the spatial distribution of ventricular Cx43 have been observed, but after treatment with SAHA, the expression of connexin40 was reduced and the distribution of connexin43 was partially normalized, solving the conduction defects [96].

Further, it has been showed by Kao and coworkers that the ejection fraction can be improved by HDAC inhibitors, with an associated decrease in the chamber size from isoproterenol-induced heart failure, which simulates dilated cardiomyopathy [97] .

AIM

Aim of the present work was to explore the impact of SERCA2 acetylation on its calcium pumping activity. Two different cell models have been used in this work, namely the HL-1 cell line, derived from atrial mice cardiomyocytes [98] submitted to the class I and II general inhibitor suberoylanilidehydroxamic acid (SAHA, or Vorinostat) and a stable cell lines (HEK cells) created to express the mutated human SERCA2 as mimicking acetylation/deacetylation on specific lysine residues. Furthermore, the recovery phase of calcium transients has been analyzed in zebrafish, normal and diabetic adult rat cardiomyocytes treated with SAHA. Notably, cardiomyocytes isolated from diabetic rat hearts have been employed because in literature it has been already demonstrated that abnormal intracellular Ca^{2+} handling can be considered one of the main pathological variations in diabetic cardiomyopathy, mostly due to a reduction in expression and activity of SERCA2 [18, 99].

In this project, we investigated the pro-acetylating effect of SAHA on SERCA2 protein and the consequent increase of the pump activity and its efficiency in cytosolic Ca^{2+} removal.

MATERIALS AND METHODS

CELLULAR MODELS

HL-1 CELLS

HL-1 cells were derived from AT-1 cardiomyocytes, that are atrial cardiac cells resultant from transgenic mouse. In this source expression of SV40 large T antigen was under control of the atrial natriuretic factor (ANF) promoter [100]. These cells maintain an adult cardiomyocyte phenotype and are able to contract spontaneously in culture; they can be recovered in frozen stocks and they can be passaged in cell culture [98]. HL-1 cardiomyocytes were characterized by using microscopic, immunohistochemical, electrophysiological, and pharmacological techniques [98]. HL-1 cells contain organized structures necessary for contraction and intracellular ANF granules typical of atrial cardiomyocytes [101], exhibit a profile similar to adult cardiomyocyte (gene expression analysis), express ion channels necessary for generation of action potentials, and undergo spontaneous depolarization [98]. Moreover, a pharmacological approach showed that HL-1 cells are able to respond appropriately to inotropic and chronotropic agents, thus suggesting that HL-1 cardiomyocytes express functional receptors (e.g. α- and β-receptors) and intracellular protein necessary for cell signaling and activation of signaling pathways. HL-1 cells have established to be an adaptable model system [101], used to explore cell signaling [102] and electrophysiology [103]. Even if HL-1 cells were originally obtained from atrial cells, they have proven to be convenient as a general model to study contracting and working cardiomyocytes, due to their organized structure and ability to contract [104] (Figure 6).

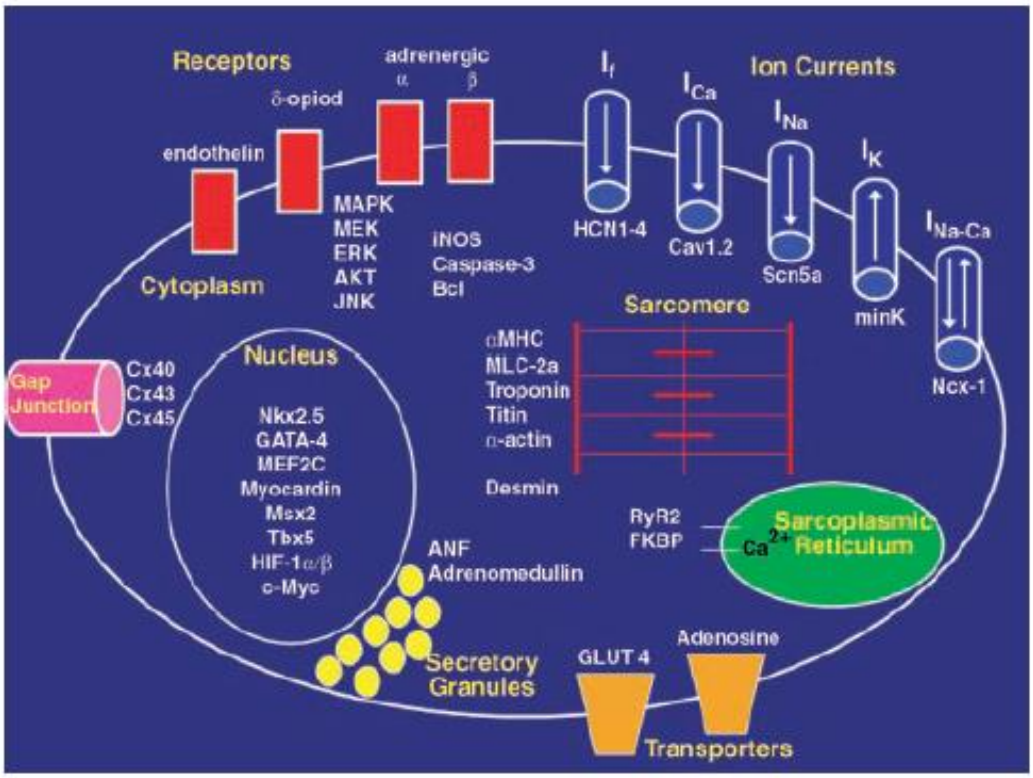

Figure 6. Schematic representation of characteristics of HL-1 cardiomyocytes. The components listed below are grouped according to their function and location within the cell.. Genes expressed in HL-1 cells are shown under the current with which they are associated *in vivo*: the sodium/calcium exchanger NCX, the modulatory β-subunit for the inward rectifier potassium current (minK), the voltage-gated sodium channel (Scn5a), the voltage-gated L-type Ca^{2+} channel (Cav1.2), and the hyperpolarization, cyclic nucleotide-gated channels HCN. Abbreviations: Cx, Connexin; iNOS, inducible Nitric Oxide Synthase; MAPK, Mitogen-Activated Protein Kinase; ERK, Extracellular signal-Regulated Kinase; MEK, MAPK/ERK kinase; JNK, Jun kinase; MHC, Myosin Heavy Chain; MLC, Myosin Light Chain; GLUT, Glucose transporter; RyR, Ryanodine Receptor; FKBP, FK506 Binding Protein; I_f, pacemaking or "funny" current; I_{Ca}, calcium current; I_{Na}, sodium current; I_K, potassium current; $I_{Na}/_{Ca}$, sodium-calcium exchange current (from Steven M. White, Phillip E. Constantin, and William C. Claycomb, Am J Physiol Heart Circ Physiol, 2004 [101]).

ADULT CARDIOMYOCYTES

Animal models have been long employed as tool to expand the knowledge of cardiac physiology and cardiac disease. The usage of isolated cardiomyocytes take a lot of advantages: it is possible to select cells from different cardiac areas, such as atrial or ventricular cells, left or right ventricle, cells belonging to the conduction system or eventually cells derived from cardiac infarcted area. Isolated cardiomyocytes are usually used to perform studies of protein biochemistry and to investigate contraction /relaxation processes and intracellular Ca^{2+} handling [105]. Adult cardiomyocytes represent an important tool in the study of cell electrophysiology and mechanics, intracellular calcium fluxes, and protein expression, thus giving to the researchers the opportunity to examine cardiac function at cellular and sub-cellular levels. Moreover, rat cardiomyocytes obtained from diabetic rat hearts have been used, based on earlier observations demonstrating that altered intracellular Ca^{2+} handling can be considered one of the major pathological changes triggering diabetic cardiomyopathy, as a consequence of a reduced expression and activity of SERCA2 [99].

The most common animal model used to study human diabetes is streptozotocin (STZ)-induced diabetes in the rat. Diabetes can be induced by destruction of the insulin-producing β-cells of the pancreas by a single injection of streptozotocin, thus simulating the signs and symptoms of chronic human type 1 diabetes, associated with early diastolic dysfunction [106]. Further, a decreased SERCA2 activity and expression can be considered as the main contributing factors to the diastolic dysfunction in heart failure and in this model of diabetes, as mentioned above [107].

Additionally, the zebrafish (*Danio rerio*) is considered an excellent model for studies relating to cardiac development and regeneration. Zebrafish heart is considered very similar to human heart, except for the notable capacity to regenerate itself after cardiac damage: in fact, zebrafish have been suggested as a good model for genetic and pharmacological analysis. Nemtsas P. and coworkers [108] characterized action potentials (APs) from intact adult atria and ventricles and found that the general profile of zebrafish APs is similar to that of humans (Figure 7). Moreover, the zebrafish action potential upstroke is controlled by Na+ channels, plateau phase is regulated by L-type Ca^{2+} and IKr channels are involved in repolarization.

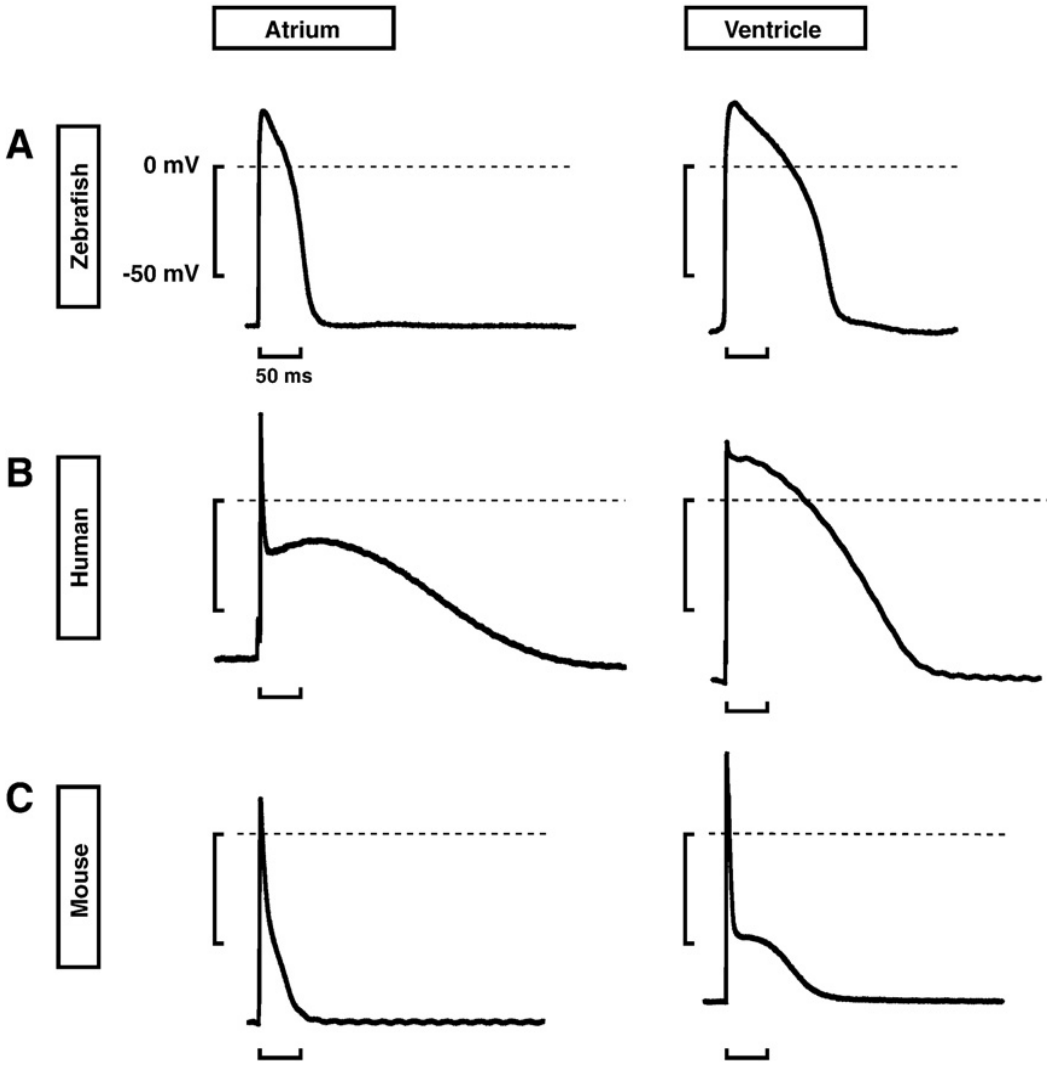

Figure 7: Representative profiles of action potentials in different species. APs in zebrafish **(A)**, human **(B)** and mouse **(C)** in atria and ventricles, at left and right columns, respectively. The overall shape of the zebrafish ventricular AP is similar to human's ventricular AP, as both of them show a plateau phase. Abbreviations: AP, Action Potential (from Nemtsas P. et al, J Mol Cell Cardiol, 2010 [108]).

HEK CELLS

Human Embryonic Kidney 293 cells (HEK 293 or HEK cells) are a specific cell line originally resulting from human embryonic kidney cells grown in tissue culture. These cells can be very easily maintained in culture and transfected.

Human embryonic kidney cells are commonly used in several experiments of transfection to induce an overexpression of single proteins. Specifically, HEK-MSR1 cells are a stable cell line produced with a plasmid expressing human Macrophage Scavenger Receptor 1, that has been shown to facilitate adhesion of cells and other cell lines to tissue culture plastic [109].
In this study HEK cells were used as hosts for gene to induce the mutated SERCA2 protein expression, where lysines (specific target of acetylation) were mutated into different amino acids to investigate the specific role of acetylation in pump ATPase function. In fact, glutamine or arginine are generally used to mimic constitutively acetylation or constitutively deacetylation because of their structure [110].

HL-1 CARDIOMYOCYTE CULTURE

HL-1 cell line was derived from the AT-1 mouse atrial cardiomyocyte tumor lineage [98]. HL-1 cells were kindly provided by Prof. W.C. Claycomb and then cultured as previously described [98] in Claycomb Medium (Sigma-Aldrich) enriched with 10% FBS (Sigma-Aldrich), 1% v/v penicillin streptomycin (Invitrogen), 2 mM L-glutamine (Invitrogen) and 100 µM norepinephrine (Sigma-Aldrich). Cells were grown at 37 °C with 5% CO_2 and 95% air. Gelatin/fibronectin-coated flasks were prepared in advance. Cells were plated at a density of 10000 cells/cm^2 and when they reached 90% confluence, culture medium was changed and supplemented with SAHA 2.5 µM (re-suspended in DMSO) for 1.5 hours. Control cells were treated with an equal amount of DMSO in culture medium.

WESTERN BLOT ANALYSIS

Cells were washed twice in PBS and then collected in protein extraction buffer (10 mM Tris-HCl pH 7.4, 150 mM NaCl, 1% Igepal CA630, 1% sodium deoxycholate, 0,1% SDS (Sodium Dodecyl Sulphate) and 1% Glycerol enriched with phosphatase and protease inhibitor mix (Roche). Proteins were then quantified by using BCA protein kit (ThermoScientific) following manufacturer's instructions. Then, 30 µg of protein extracts were loaded on precast gradient (4-12%) gels (Invitrogen) and separated by SDS-PAGE using MOPS running buffer (Invitrogen). Proteins were moved onto nitrocellulose membranes or PVDF (Bio-Rad) in Transfer buffer (Life Technologies) supplemented with 10% (v/v) methanol. Membranes were blocked in 5% non-fat dry milk or 5% BSA in PBS containing 0.05% Tween20 (1 hour at room temperature), and then incubated overnight at 4°C with primary antibodies: SERCA2 (1:1000, Santa Cruz, sc-376235), Ac-α-tubulin (1:1000, Sigma-Aldrich #T6793), α-tubulin (1:2000, Sigma-Aldrich #T9026) and β-actin (1:5000, Sigma-Aldrich, #A5441). Three washes were performed with 1× PBS-Tween buffer ten minutes each at room temperature and then membranes were incubated with horseradish peroxidase conjugated secondary antibody (SantaCruz) for 1 hour at room temperature. Signal was detected with enhanced chemiluminescence system (Supersignal West Dura Extended Duration Substrate, ThermoScientific) and results were quantified by ImageJ 1.48 software.

IMMUNOPRECIPITATION

Co-Immunoprecipitation was done by using protein-Agarose accordingly to the manufacturer's instructions (Roche). Specifically, 4 µg of anti-SERCA2 or anti-acetyl Lysine (Cell Signaling #9441) antibodies were co-immunoprecipitated with 500 µg of proteins. Negative controls were performed with the equal amount of protein extract, obtained from HL-1 cells not treated, precipitated with the corresponding purified IgG antisera (SantaCruz) without primary antibody. Samples were then separated by SDS–PAGE and both transfer and blotting procedures were performed as described in the western blot paragraph.

CELL IMMUNOFLUORESCENCE

HL-1 cells were fixed in 4% PFA for 10 min at room temperature. Permeabilization was performed with 0.2% Triton X-100 for 5 min at room temperature and blocking was conducted for 1 h at room temperature with PBS supplemented with 5% goat serum. Cells were then incubated overnight at 4°C with a mouse polyclonal anti-SERCA2 antibody (Santa Cruz, sc-376235) (dilution 1:200) in PBS with 2% goat serum. Cells were washed three times with PBS for 10 minutes and then incubated for 1 h at 37°C with the FITC-conjugated goat anti-mouse secondary antibody (dilution 1:200) diluted in PBS with 2% oat serum. Nuclei were counterstained with Hoescht 33342 (Sigma-Aldrich) and epifluorescent signals were detected by using a Zeiss Axioskop II optical microscope.

INCX MEASUREMENTS

HL-1 cells were grown as described above. When cells reached confluence, they were enzymatically dissociated and treated with 2.5 μM SAHA or DMSO for 90 minutes. INCX was recorded in the whole-cell configuration of the patch-clamp technique. Briefly, cells were located on the platform of an inverted microscope (Nikon Eclipse Ti) and measurements were recorded with a patch amplifier (Axopatch 700B; Molecular Devices), signals were detected by using a DAC/ADC interface (Digidata 1550; Molecular Devices) and data obtained by means of PClamp software (Vers. 10, Molecular Devices). Patch pipettes had a resistance of 3-4 MΩ when filled with the internal solution (in mM: 120 CsCl, 3 CaCl2, 0.5 MgCl2, 20 HEPES, 5 Mg-ATP, 5 BAPTA K+4). Cells were superfused with the external solution (in mM: 128NaCl, 10 CsCl, 2 CaCl2, 1 MgCl2, 10 HEPES, 10 D(+)-glucose, 0.01 Lacidipine, 0.1 SITS, 0.0005 Ouabain, pH 7.2 with CsOH). INCX was documented in voltage-clamp mode by applying a ramp voltage protocol starting from -120 mV to +50 mV, by adding to the external solution 5 mM of NiCl2 to block specifically INCX. Experiments were conducted at 26±2 °C and the INCX was calculated as a difference of nichel sensitive current. Further, INCX density current was calculated by dividing the current by cell membrane capacitance (Cm), designed by applying a ± 10 mV pulse starting from a holding potential of -70 mV, as previously reported [103]. Analysis of INCX was performed with pClamp10.0/Clampfit (Molecular Devices) and Origin 9.1 (Origin lab Corporation).

REAL TIME RT-PCR

For gene expression study, RNA was obtained using TRIzol reagent. 1 µg of RNA was reversely transcribed with SuperScript® VILO cDNA Synthesis Master Mix (Invitrogen). cDNA was then amplified with SYBR-GREEN quantitative PCR on CFX96™ Real-Time PCR Detection System (Bio-Rad). Five candidate housekeeping genes, among different usually used ones, were explored in order to choose the most stable in HL-1 cell model: β-Actin (ACTB), TATA box binding protein (TBP), glyceraldehyde-3-phosphate dehydrogenase (GAPDH), hypoxanthine guanine phosphoribosyl transferase (HPRT) and β-2 microglobulin (B2M). NormFinder software [111] was used to recognize the optimal normalization gene among the different candidates. B2M resulted as the most appropriate housekeeping gene for SERCA2a expression study. The following primers for mouse SERCA2a and B2M were used:

- SERCA2a fw 5′-TCGACCAGTCAATTCTTACAGG-3’
- SERCA2a rev 5′- CAGGGACAGGGTCAGTATGC-3’
- B2M fw 5′- GGAAGCCGAACATACTGAACTG-3’
- B2M rev 5′-TCCCGTTCTTCAGCATTTGG-3’.

Raw expression intensities of SERCA2a were normalized to the Ct value of B2M, chosen as internal control. Relative quantitation was calculated by using the ΔΔCt method in comparison to not treated cells and fold changes in gene expression were estimated as $2^{(-\Delta\Delta Ct)}$ [112].

ISOLATION OF THE MICROSOMAL FRACTION

Microsomes were isolated from HL-1 cells and rat heart cardiomyocytes in according to Maruyama and MacLennan [113] with minor modifications. Specifically, cells were washed with cold PBS and then homogenized with 30 strokes in a glass Dounce homogenizer. The resulted homogenate was diluted with an equal volume of a solution of 0.5 M sucrose/ MgCl2 Tris-HCl, pH 7.5. Samples were centrifuged at 10,000 x g for 20 min at 4°C to pellet nuclei and mitochondria. Pellet was discarded and the supernatant was centrifuged at 100,000 x g for 60 min at 4°C to obtain the microsomal fraction, that was re-suspended in a solution containing 0.25 M sucrose and 10 mM MOPS. All solutions were supplemented with protease inhibitors (Roche). Microsomes

were stored at -80° in several aliquots after measurement of concentration, performed by BCA protein kit (ThermoScientific), following manufacturer's instructions.

ATP/NADH COUPLED ASSAY FOR CALCIUM ATPASE ACTIVITY

The assay is based on the reaction in which the regeneration of hydrolysed ATP is coupled to the NADH oxidation. Following ATP hydrolysis, the regeneration system comprising of phosphoenolpyruvate (PEP) and pyruvate kinase (PK) transforms one molecule of PEP to pyruvate while ADP is converted to ATP. Pyruvate is then transformed to lactate by L-lactate dehydrogenase (LDH) resulting in the oxidation of one NADH molecule (all reagents are from SIGMA). The rate of NADH absorbance decrease at 340 nm and it is proportional to the rate of steady-state ATP hydrolysis. The continuous regeneration of ATP allows the monitoring of the ATP hydrolysis rate over the entire course of the assay. Activity of the calcium ATPase was then calculated as Δabsorbance/6,22*protein*time (μmol P/min/mg protein) [55]. Calcium ATPase activity of HL-1 cells was measured from 30 μg of microsomes in each cuvette by using a Beckman DU-640 spectrophotometer, whereas the ATPase activity of rat cardiomyocytes was revealed from 4 μg/well by performing the assay in microplate and by measuring the absorbance with Envision multilabel reader (Perkin Elmer).

BIOINFORMATIC ANALYSIS

Different post-translation modification databases (PHOSIDA and scan-x) were used to identify candidate acetylation sites on human SERCA2a sequence. Structural models of human SERCA2a for the four different functional states were generated by comparative modeling using MODELLER, based on rabbit SERCA1 template structures that have been determined experimentally by X-ray diffraction. Rabbit SERCA1 is a close homologue to human SERCA2a with 83% sequence identity. The modelling was performed to investigate the potential impact of lysine acetylation on SERCA2a function. In particular the candidate acetylation sites were analyzed in relation to their location in the structure, their accessibility and proximity to functional sites. PHOSIDA is another phosphorylation site database: it permits the investigation of phosphorylation, acetylation and N-glycosylation data of the protein of interest. Additionally, it shows structural and evolutionary information on modified proteins [114].
Scan-x is a software tool planned to identify motifs within any sequence [115, 116].

MODELLER was used for homology or comparative modeling of three-dimensional structures of proteins [117, 118]. MODELLER generates a structural a model of the protein of interest based on an alignment to a template structure.

MUTAGENESIS

SERCA2a mutants were generated by PCR-site directed mutagenesis and verified by complete sequencing (Eurofins MWG). The SERCA2a wild-type coding sequence (SERWT) as well as the SERCA2a coding sequence with the K residues mutated into Glutamine (SERKQ) or Arginine (SERKR) were subsequently cloned into in the pCDNA3 vector (Life Technologies) for cell transfection (for primers' list see table 5). Transient transfections were performed on HEK-MSR1 cell line with Lipofectamine LTX (Invitrogen) following manufacturer's instructions. Stable cell lines were then generated 24 hours after transfections with culture medium supplemented with Geneticin, the selection agent whose resistance was included in the pCDNA3 plasmid.

SERWT-F	AAAGGTACCATGATGGAGAACGCGCACACCAAGACG
SERWT-R	TTTGGGCCCTTACTCCAGTATTGCAGGTTCCAGGTAG
K464Q-F	GAAGGGTCTTTCTCAGATAGAACGTGC
K464Q-R	GGCATTTGCACGTTCTATCTGAGAAAGACC
K464R-F	GAAGGGTCTTTCTAGAATAGAACGTGC
K464R-R	GGCATTTGCACGTTCTATTCTAGAAAGACC
K585R-F	GCCAACTTTATTAGATATGAGACCAATCTG
K585R-R	TCAGATTGGTCTCATATCTAATAAAGTTGG
K585Q-F	GCCAACTTTATTCAGTATGAGACCAATCTG
K585Q-R	TCAGATTGGTCTCATACTGAATAAAGTTGG

Table 5: Primers list

ZEBRAFISH POPULATION

Zebrafish were maintained at 28.5°C in 14:10 hours light/dark conditions, 50 adults/10 L tank according to standard methods [119].
All procedures adhered to the guidelines from the Italian Ministero della Sanità, Office of the Animals Scientific Procedures.

ZEBRAFISH CARDIOMYOCYTE ISOLATION

Enzymatic dissociations were performed to isolate adult zebrafish cardiomyocytes as previously described [120]. After removal, hearts of 5 zebrafish (for each experiment) were washed twice in a buffer containing PBS, 5.5 mM glucose, 10 mM HEPES, 10 mM 2,3-butanedione monoxime (BDM) and 30 mM taurine and then located into digestion buffer (perfusion buffer supplemented with 12.5 µM $CaCl_2$ and 0.2 Wünsch units/ml Liberase Blendzyme 3 (Roche). Two following digestions occurred at 27ºC in a thermomixer at 800 rpm for 40 minutes. Digestions were interrupted by using digestion buffer with 10% FBS. Calcium restoration was completed by raising different concentrations: 0.125, 0.250, 0.500 mM, respectively. Cardiomyocytes were then used to measure calcium transients by using IonOptix fluorescence and contractility system.

RAT POPULATION

This study was carried out in accordance with the recommendations included in the Guide for the Care and Use of Laboratory Animals of the National Institutes of Health. The protocol was approved by the Committee on the Ethics of Animal Experiments of the University of Parma. All efforts were made to minimize animal suffering.
15 male Wistar rats (*Rattus norvegicus*), aged 12-14 weeks and weighing 362±5 g, were individually housed in a temperature-controlled room at 22–24 °C, with the light on between 7.00 AM and 7.00 PM. 6 animals were exposed to a single intra-peritoneal injection of Streptozotocin (60 mg/kg) to induce diabetes, whereas 8 control rats were injected with saline vehicle (0.9% NaCl). Body weights and glucose blood levels were measured in 4-hour-fasting animals, before STZ or vehicle injection, two days after injection, and then weekly until sacrifice, three weeks after injection.

RAT CARDIOMYOCYTE ISOLATION

Ventricular myocytes were enzymatically isolated by perfusion from the hearts of control and diabetic rats, as previously described [121]. Briefly, rats were anesthetised with ether approximately for five minutes and the heart was removed and rapidly perfused at 37°C through an aortic cannula with the following sequence of solutions:

- a calcium-free solution for 5 min to remove the blood; calcium-free solution contained the following (in mM): 126 NaCl, 22 dextrose, 5.0 $MgCl_2$, 4.4 KCl, 20 taurine, 5 creatine, 5 sodium pyruvate, 1 NaH_2PO_4, and 24 HEPES (pH 7.4, adjusted with NaOH, and gassed with 100% O_2)
- a low-calcium solution (0.1 mM) plus 1 mg/ml type 2 collagenase (Worthington Biochemical) and 0.1 mg/ml type XIV protease (Sigma) for about 20 min;
- an enzyme-free, low-calcium solution for 5 min.

The left ventricle was then minced and shaken for 10 min. Cells were filtered through a nylon mesh and re-suspended in low-calcium solutions (0.1 mM) for 30 min. Before measuring cell mechanics, cells were incubated with SAHA 2.5 nM for 90 min. A subgroup of control and diabetic cardiomyocytes, after SAHA incubation, were loaded with 10 μM Fluo 3-AM (Invitrogen) for 30 min to measure calcium transients simultaneously with mechanical properties by using IonOptix fluorescence and contractility systems (IonOptix). For each group, cell mechanics and calcium transients were also recorded from untreated ventricular myocytes.

RAT CARDIOMYOCYTE CONTRACTILITY MEASUREMENTS

Cardiomyocytes were placed in a chamber mounted on an inverted microscope (Nikon-Eclipse TE2000-U, Nikon Instruments) and perfused (1ml/min at 37°C) with a Tyrode solution containing (in mM): 140 NaCl, 5 HEPES, 1 $MgCl_2$, 5.4 KCl, 5.5 glucose, and 1 $CaCl_2$ (pH 7.4, adjusted with NaOH). Only rod-shaped cardiomyocytes with pure edges and a sarcomere length $\geq$ 1.7 μm were designated for the analysis. All selected cardiomyocytes did not show any spontaneous contractions. Cells were field stimulated at a frequency of 0.5 Hz by constant current pulses (2 ms in duration, and twice diastolic threshold in intensity) carried by platinum electrodes placed on opposite sides of the chamber, connected to a MyoPacer Field Stimulator (IonOptix). Cells were displayed

on a computer monitor using an IonOptix MyoCam camera. Load-free contraction of myocytes was measured with the IonOptix system, which detected sarcomere length dynamics through a Fast Fourier Transform algorithm. The following parameters were computed: mean diastolic sarcomere length, fraction of shortening (FS), maximal rates of shortening and re-lengthening ($\pm dL/dt_{max}$), time to peak of shortening (peak-T), and time at 50% and 90% of re-lengthening (time to RL 50%, time to RL 90%, respectively). Steady-state contraction of cardiomyocytes was reached before data recording by means of a 10 seconds conditioning stimulation.

CALCIUM TRANSIENTS

ADULT CARDIOMYOCYTES

Adult zebrafish and rat cardiomyocytes were treated for 1.5 hs with SAHA 2.5 µM and 2.5 nM, respectively. Cells were loaded with 10 µM Fluo 3-AM (Invitrogen) for 30 min. Calcium transients were induced by a field stimulation at a frequency of 0.5 Hz and measured by the IonOptix Myocyte Calcium and Contractility Recording System. Adult zebrafish cardiomyocytes were perfused with Tyrode's solution containing in mM: D(+)-glucose 10, Hepes 20, NaCl 126, KCl 5.4, $MgCl_2$ 5, $CaCl_2$ 1 (pH adjusted to 7.4 with NaOH), whereas adult rat cardiomyocytes were perfused with a Tyrode's solution containing in mM: 140 NaCl, 5.4 KCl, 1 $MgCl_2$, 5 HEPES, 5.5 glucose, and 1.8 $CaCl_2$ (pH 7.4, adjusted with NaOH).

Calcium transients were defined by epifluorescence: excitation length was 480 nm, with emission length at 535 nm. Fluo-3 signals were expressed as normalized fluorescence (F/F_0, fold increase). The maximal rate of fluorescence decline and the time to 50% and 90% of fluorescence decay (corresponding to the recovery phase of calcium transients) were computed, thus resulting in different parameters: time to baseline (BL) 50% and 90%. The time course of the fluorescence signal decay was defined by a single exponential equation and the time constant (tau) was used as a measure of the rate of intracellular calcium clearing [21]. Traces were then analyzed with Ionwizard software.

SERCA2 MUTANTS

HEK-MSR1 stably transfected (as described above) with K464 and K585 onto SERCA2 sequence mutated in Q or R were plated on the bottom of glass dishes (25 mm diameter) and grown for 2 days in MEM medium supplemented with 10% FBS, 2 mM L-glutamine, MEM Non-Essential Amino Acids Solution (100X) and 50 µg/mL Geneticin. Cytosolic Ca^{2+} dynamics were analyzed in Fluo 4-AM loaded cells. Briefly, cells were loaded with 5 µM of Fluo4-AM (Molecular Probes-Invitrogen Life Technologies) for 20 min at room temperature and then washed with Tyrode's solution containing in mM: D(+)-glucose 10, NaCl 140, Hepes 5.0, $MgCl_2$ 1.2, KCl 5.4, $CaCl_2$ 1.8 (pH adjusted to 7.3 with NaOH). Dishes were placed in a perfusion chamber of an epifluorescence microscope (Nikon Ti) equipped with a 75 W Xenon lamp and connected to a CCD camera (Cool SnapTM EZ Photometrics). Cells were excited at 488 nm wavelength and the fluorescence emission was measured at 520 nm and recorded using the MetaFluor Software (Molecular Devices). Imaging was scanned constantly at 80 ms interval. 10 mM caffeine-pulse was used to evoke calcium transients. Experiments were conducted at 36.5 ± 0.5°C. A signal-to-noise ratio of at least 50 arbitrary unit (A.U.) was considered as Ca^{2+} signal.

Traces were resampled uniformly at 5Hz using an RBF interpolator (s=1, k=3) to remove noise. Baseline was considered by calculating the median value of the first 2 seconds before the excitation. By scaling the traces from baseline/peak, the time to decay at the first intersection of 50, 90% of the curves was calculated, thus defining time to BL 50% and 90% as described in the above paragraph.

STATISTICAL ANALYSIS

Data were denoted as means ± sem. Statistical analysis were performed using unpaired two-tailed Student t-test when appropriate or One-way ANOVA, followed by Bonferroni's multiple comparison test (in figure legend, test used for each specific experiment is reported). A p-value < 0.05 was considered statistically significant.

RESULTS

EFFECT OF SAHA TREATMENT ON HL-1 CARDIOMYOCYTES

HL-1 cell line is a line derived from atrial mouse cardiomyocytes, capable to contract and partially retain an adult cardiac phenotype [98]. As established by immunofluorescence and Western Blot techniques, they are able to express the cardiac isoform 2 of the Sarco/Endoplasmic Reticulum Calcium ATPase (SERCA) (Figure 8A and 8B). As expected, SERCA1 is expressed in rat skeletal muscle and not in mouse total heart. Further, it has been reported that SERCA3 is expressed in non-muscle cells, so it is not present in any samples analyzed [6].

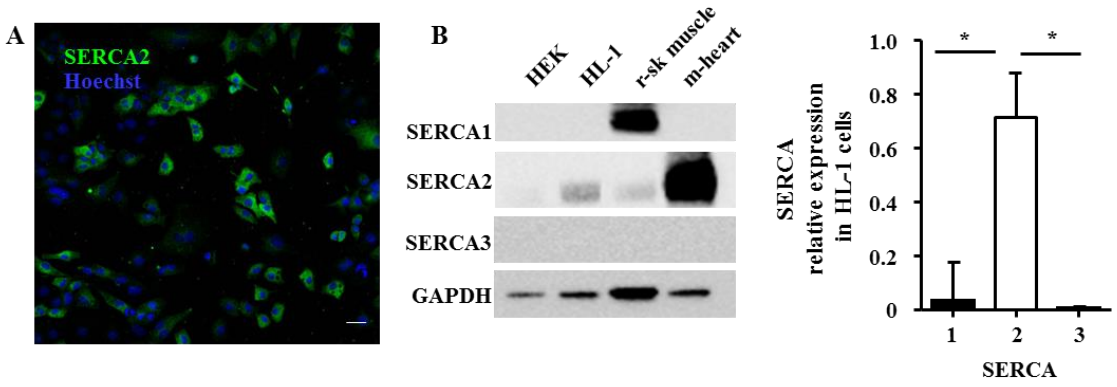

Figure 8: SERCA2 expression in HL-1 cells. (A) Immunofluorescence assays performed on HL-1 cells. Nuclei were counterstained with Hoechst (blue). Scale bar = 50 µm. **(B)** Western blot analysis performed on different lysates showed SERCA2 expression only in HL-1 cells and in mouse heart (n=3). Densitometric analysis is on the right. Data are presented as mean ± sem, One-way ANOVA, followed by Bonferroni's multiple comparison correction, * $p < 0.05$ vs SERCA2..

The treatment of HL-1 cells with the pan-inhibitor of class II HDAC SAHA 2.5 µM for 1.5 hours (suberanilohydroxamic acid) allowed an increase in acetylation of SERCA2, demonstrated by co-immunoprecipitation experiments (Figure 9A). It has been detected, as a positive control of the effect of HDAC inhibition, also the increase of acetyl-α-tubulin levels after SAHA treatment (Figure 9B). Importantly, SERCA2 expression

both at protein and mRNA levels did not change after SAHA adjunct, as reported in figure 9B and 9C, by performing western blot and real-time RT-PCR experiments. Notably, the concentration of SAHA 2.5 μM used in these experiments did not provoke significant cell death or signs of cell suffering (Figure 9D).

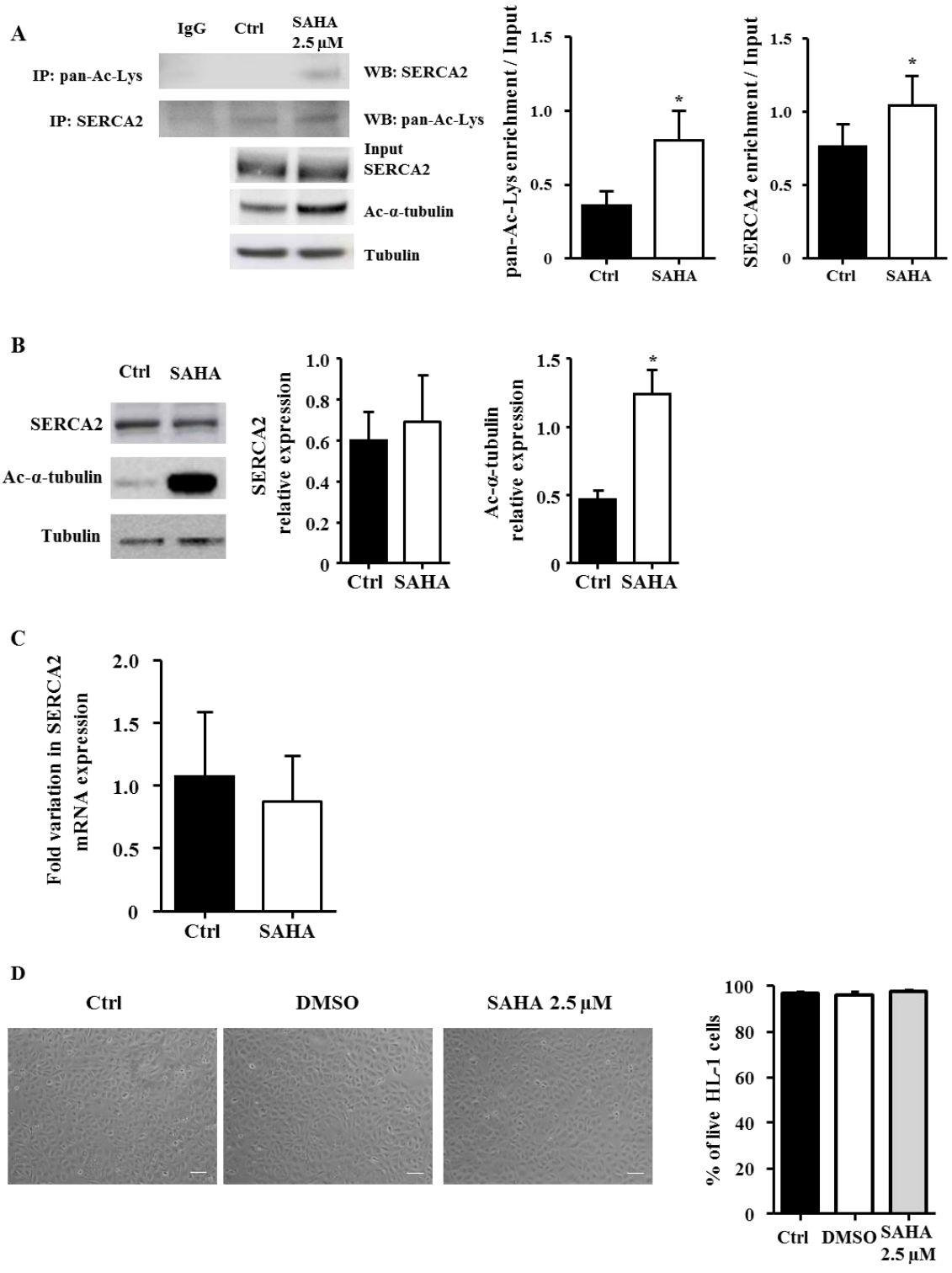
A
IgG
Ctrl
SAHA 2.5 µM
IP: pan-Ac-Lys
WB: SERCA2
IP: SERCA2
WB: pan-Ac-Lys
Input SERCA2
Ac-α-tubulin
Tubulin
pan-Ac-Lys enrichment / Input
SERCA2 enrichment / Input
Ctrl
SAHA
B
Ctrl
SAHA
SERCA2
Ac-α-tubulin
Tubulin
SERCA2 relative expression
Ac-α-tubulin relative expression
C
Fold variation in SERCA2 mRNA expression
D
Ctrl
DMSO
SAHA 2.5 µM
% of live HL-1 cells

Figure 9: HDAC inhibition allowed Serca2 acetylation. (A) Immunoprecipitation experiment showing SERCA2 acetylation increases after SAHA exposure (n=3). Densitometries are on the right. Data are presented as mean ± sem, unpaired Student t-test: * $p < 0.05$ vs Ctrl. **(B)** Ac-α-tubulin expression analyzed by Western blot in HL-1 cells whole cell lysates not treated and treated with SAHA (2.5 µM) for 1.5 hours (n=3). Densitometric analysis is on the right. Data are presented as mean ± sem, unpaired Student t-test: * $p < 0.05$ vs Ctrl. **(C)** Real time RT-PCR for SERCA2a mRNA expression in HL-1 cells treated and not treated with SAHA 2.5 uM (n=3). Data are presented as mean ± sem, unpaired Student t-test. **(D)** HL-1 cells not treated (left) and treated with SAHA 2.5 µM (right) and equal amount of DMSO (middle) and corresponding cell count of viable cells with trypan blue (scale bar = 50 µm; graph on the right; n=3). Data are presented as mean ± sem, One-way ANOVA, followed by Bonferroni's multiple comparison correction.

Furthermore, to study whether SAHA treatment, and consequently HDAC inhibition, could affect SERCA2 pump activity, microsomes were isolated from HL-1 cells. Microsomes are vesicle-like artifacts obtained from pieces of the sarco-endoplasmic reticulum (SR). After several differential centrifugations, purified portions of membranes were obtained. SERCA2 was expressed only in microsomes purified fraction and not in supernatant, as confirmed by Western Blot analysis (Figure 10A). SERCA2 activity was detected by performing ATP/NADH coupled assay on microsomes isolated from HL-1 cells not treated and treated with SAHA, showing that SAHA treatment promoted a significant increase of pump activity at different calcium concentration (Figure 10B). To investigate the involvement of NCX, the specific current was quantified as Ni^{2+}-sensitive current in response to a voltage ramp in HL-1 cells. HDAC inhibition promoted by SAHA did not affect the NCX current at the different membrane potentials analyzed, from -80 mV to 30 mV (Figure 11A and B).

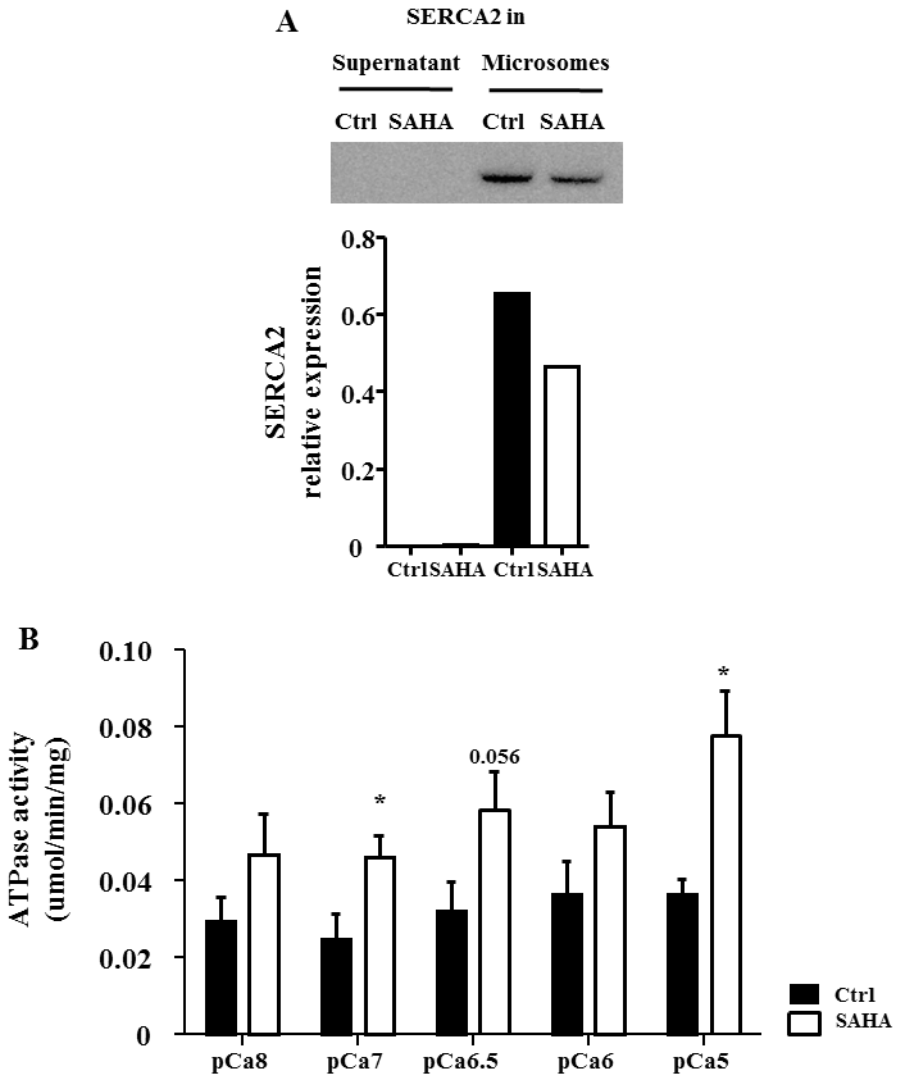

Figure 10: SERCA2 expression and activity in microsomes isolated from HL-1 cells. (A) Western blot analysis on microsomes isolated from HL-1 cells contained an higher content in SERCA2 protein than supernatant fraction (n=1). **(B)** SERCA2 activity measured by NADH-ATP coupled assay in microsomes isolated from HL-1 cells not treated and treated with SAHA (n=5). Data are presented as mean ± sem, unpaired Student t-test: * $p < 0.05$ vs Ctrl.

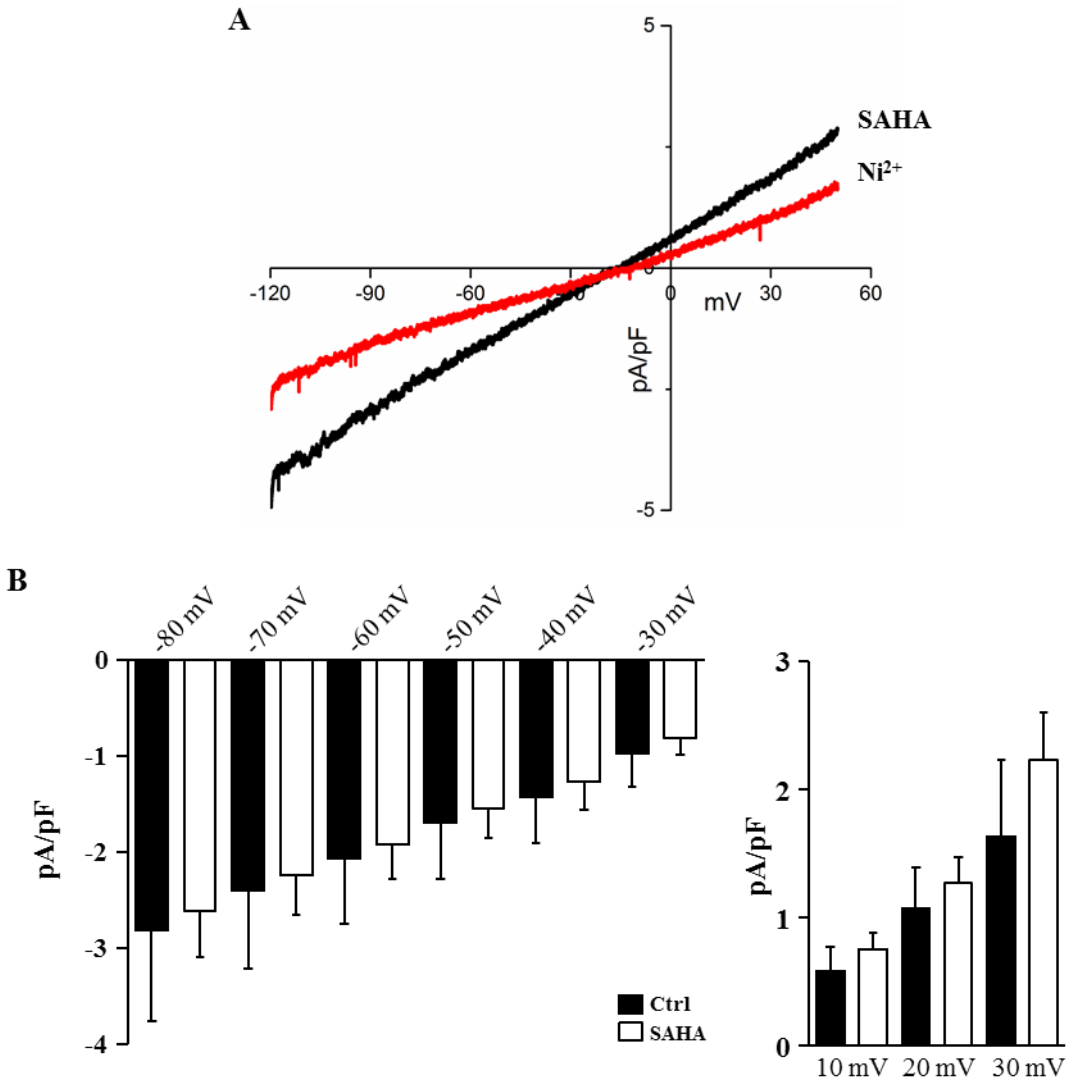

Figure 11: NCX current is not affected after SAHA treatment in HL-1 cells. (A) Typical Nichel sensitive NCX current recording after SAHA treatment in HL-1 cells. **(B)** NCX density current measured at different voltage potential (Ctrl=11, SAHA=18). Data are presented as mean ± sem, unpaired Student t-test.

EFFECT OF SAHA TREATMENT ON ISOLATED HEALTHY CARDIOMYOCYTES

In order to investigate whether pro-acetylation treatments can improve cardiac function by acting at the single cell level, we decided to analyze parameters related to contraction and calcium dynamics on cardiomyocytes enzymatically isolated from adult healthy rats. This kind of cells resulted very sensitive to SAHA contact. In fact, 2.5 µM SAHA, used before for HL-1 cells, significantly induced cells death while the application of SAHA 2.5 nM did not induce cell suffering. Measurements of cell mechanics revealed that SAHA 2.5 nM treatment enhanced re-lengthening time measured at 90% of the initial cell length (time to RL 90%, figure 12), even if there was no effect on calcium transients.

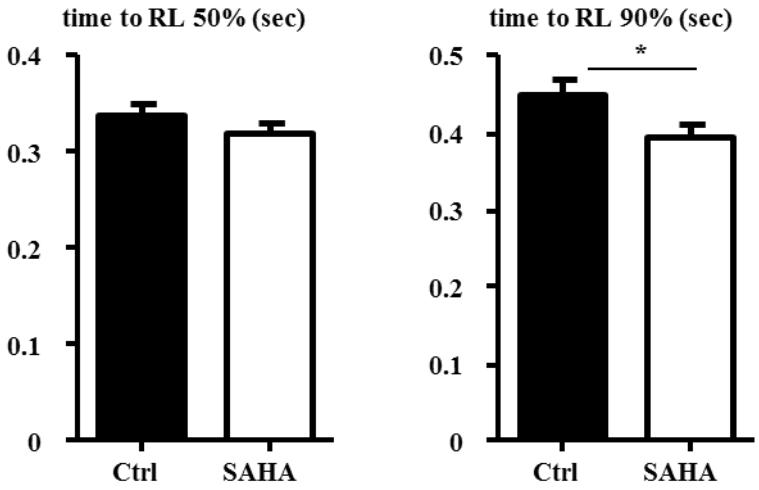

Figure 12: Contraction parameters on isolated rat cardiomyocytes. Time to 50% and 90% of re-lengthening measured in adult rat cardiomyocytes not treated and treated with SAHA 2.5 nM for 1.5 h (Ctrl = 58, SAHA = 42). Data are presented as mean ± sem, unpaired Student t-test: * $p < 0.05$ vs Ctrl.

Interestingly, the treatment with SAHA 2.5 µM of adult isolated zebrafish cardiomyocytes did not promote cell suffering (Figure 13) and induced a significant reduction in time to BL 50% and time to BL 90%, thus ameliorating the efficiency of cytosolic calcium clearing mechanisms (Figure 14).

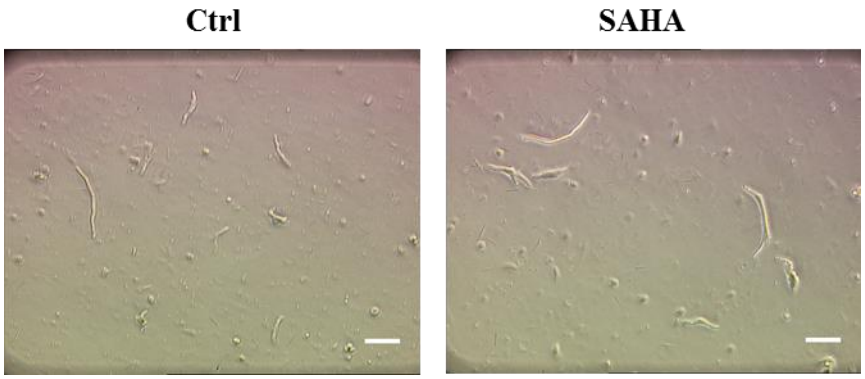

Figure 13: Isolated zebrafish cardiomyocytes. Control cardiomyocytes (left) and treated with SAHA 2.5 µM for 1.5 h (right; scale bar = 50 µm).

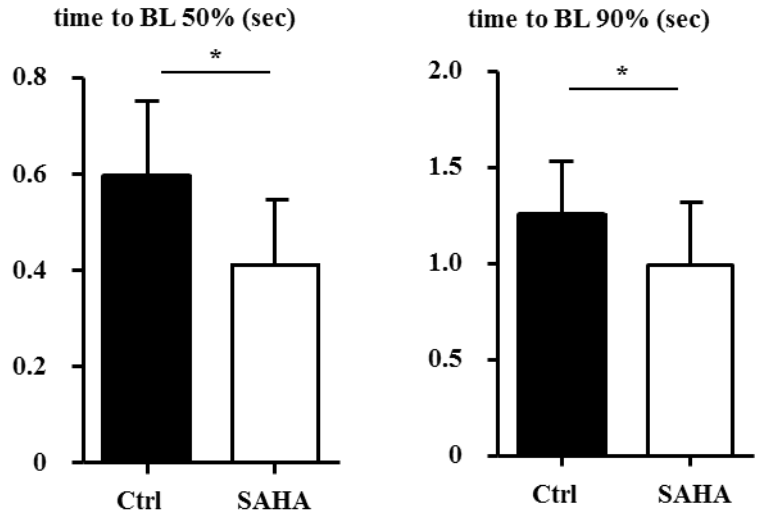

Figure 14: SAHA effect on calcium transients in adult zebrafish cardiomyocytes. Adult zebrafish cardiomyocytes treated with SAHA 2.5 µM for 1.5 h showed a significant shortening of recovery time of calcium transients, measured at 50% (left) and 90% (right) of decay (Ctrl n=26, SAHA n=11; field stimulation at 0.5 Hz). Data are presented as mean ± sem, unpaired Student t-test: * $p < 0.05$ vs Ctrl.

EFFECT OF SAHA TREATMENT ON CMS ISOLATED FROM DIABETIC RAT HEARTS

As expected, on microsomes isolated from diabetic rat cardiomyocytes SERCA2 function was decreased. Nevertheless, accordingly with our hypothesis, SAHA treatment which induced the HDAC inhibition, resulted in a significant increase in SERCA2 activity, thus rescuing its function (Figure 15).

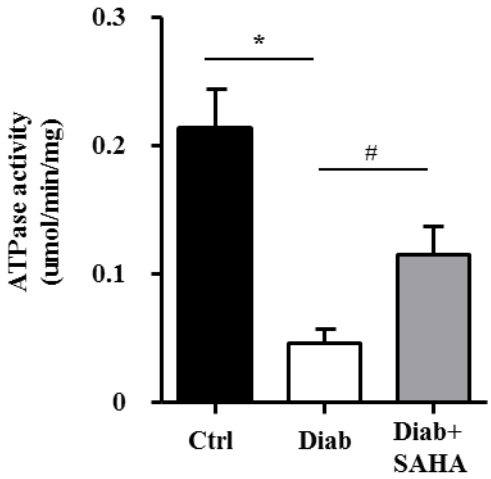

Figure 15: SERCA2 activity rescue after SAHA treatment in microsomes isolated from diabetic rat cardiomyocytes. Calcium ATPase activity is decreased in diabetic cells, but SAHA treatment induced a more efficient reuptake of calcium into sarcoplasmic reticulum (n=4). Data are presented as mean ± sem, One-way ANOVA, followed by Bonferroni's multiple comparison correction, * $p < 0.05$ vs Ctrl; # $p < 0.05$ vs Diab. Each measurement was performed in triplicate.

Notably, cardiomyocytes isolated from streptozotocyn-induced diabetic rat hearts showed a substantial worsening of cell mechanical properties and intracellular calcium dynamics compared to control samples. In diabetic cardiomyocytes, the significant reduction in the fraction of shortening was linked with a decrease in the maximal rate of shortening (-dL/dtmax) and re-lengthening (+dL/dtmax,), leading to an overall prolongation of contraction/re-lengthening times. The compromised contractility was associated with an altered calcium handling, including a significant increase in the time required for cytosolic calcium removal, such as time to BL 50%, time to BL 90% and tau (Figure 16, left, middle and right, respectively).

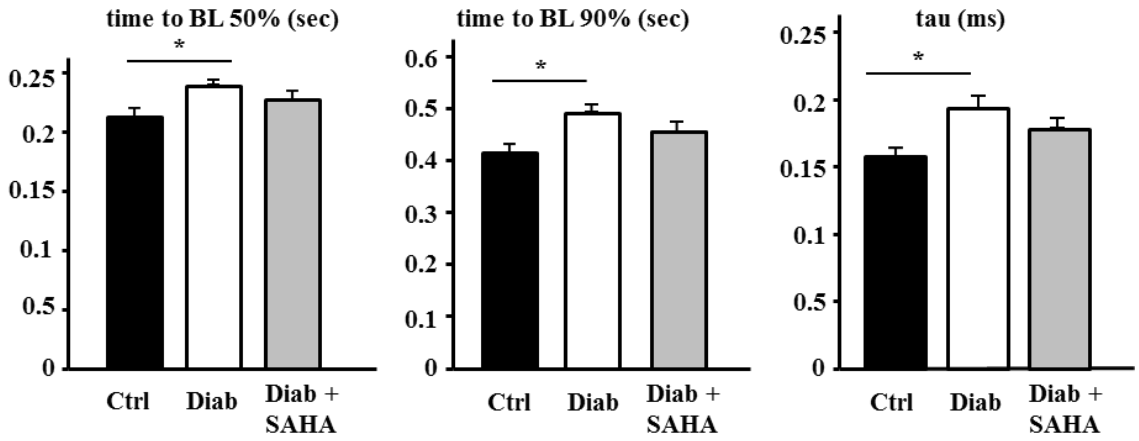

Figure 16: Recovery phase of calcium transients in diabetic cardiomyocytes treated with SAHA is faster. Calcium transients analysis in diabetic rat cardiomyocytes (±SAHA 2.5 nM for 1.5 h) revealed that SAHA treatment rescued time to BL 50% and time to BL 90% after field stimulation at 0.5 Hz (left and middle, respectively). Tau is also decreased after HDAC inhibition (ctrl n=35, Diab n=36, Diab+SAHA=34). Data are presented as mean ± sem, One-way ANOVA, followed by Bonferroni's multiple comparison correction, * $p < 0.05$.

The action of SAHA 2.5 nM was effective in rescuing near to control values the kinetic constant (tau) and the time to BL 50% and time to BL 90% of calcium transients (Figure 16), associated to the fraction of shortening, the maximal rate of shortening and re-lengthening, and the time to RL 90% (Figure 17).

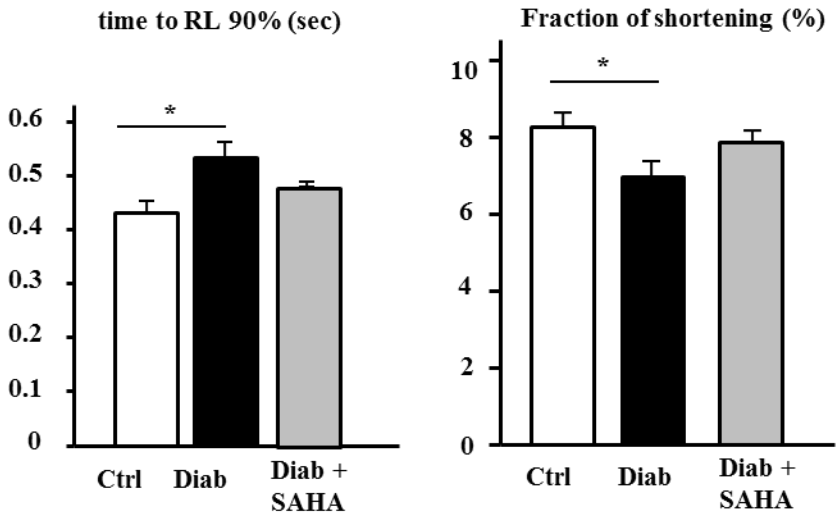

Figure 17: Contraction parameters of diabetic cardiomycytes ameliorated after SAHA exposure. Time to RL 90% and fraction of shortening (left and right, respectively) of diabetic cardiomyocytes tend to rescue after treatment with SAHA. (Ctrl n=35, Diab n=36, Diab+SAHA=34, field stimulation at 0.5 Hz). Data are presented as mean ± sem, One-way ANOVA, followed by Bonferroni's multiple comparison correction, * $p < 0.05$ vs Ctrl.

PREDICTION OF PUTATIVE LYSINE ACETYLATION SITES OF HUMAN SERCA2A

The results described above are in line with the supposition that direct acetylation can increase mouse SERCA2 (mSERCA2) activity. In support of these results, the free on-line program PHOSIDA (www.phosida.org) was used to investigate putative conserved lysine acetylation sites in human protein sequence and then checked the site conservation among SERCA2 orthologues in different species (from *Danio rerio* to *Homo sapiens*; Table 6). This analysis showed that at least 5 consensus sequence for lysine acetylation were conserved among different species, including K262, K297, K464, K514 and K585. Considering that also NCX is involved in calcium removal, we performed the same prediction analysis, but putative acetylation lysines onto NCX sequence were less conserved in considered species (Table 7).

Species	Putative conserved Nε-lysine acetylation sites in SERCA2 sequence					
Danio rerio	K262 (92%)	K297 (91%)	K436 (91%)	K464 (95%)	K515 (92%)	
Mus musculus	K262 (92%)	K297 (92%)		K464 (91%)	K514 (92%)	K585 (92%)
Rattus norvegicus	K262 (92%)	K297 (92%)		K464 (91%)	K514 (92%)	K585 (92%)
Cavia porcellus (predicted)	K262 (92%)	K297 (92%)		K464 (91%)	K514 (92%)	K585 (92%)
Canis lupus familiaris	K262 (92%)	K297 (92%)		K464 (91%)	K514 (92%)	K585 (92%)
Sus scrofa	K262 (92%)	K297 (92%)		K464 (91%)	K514 (92%)	K585 (92%)
Homo sapiens	K262 (92%)	K297 (92%)		K464 (91%)	K514 (92%)	K585 (92%)

Table 6: Putative Lysines acetylation sites in SERCA2 sequence in different species. Prediction was performed by using free software PHOSIDA.

Species	Putative conserved Nε-lysine acetylation sites in NCX sequence					
Danio rerio	K259 (100%)	K263 (87%)		K694 (91%)	K751 (91%)	
Mus musculus	K257 (100%)	K261 (91%)	K572 (91%)		K725 (92%)	K783 (91%)
Rattus norvegicus	K257 (100%)	K261 (91%)	K572 (91%)		K726 (92%)	K784 (91%)
Cavia porcellus	K257 (100%)	K261 (91%)	K650 (93%)	K650 (93%)	K725 (92%)	K783 (91%)
Canis lupus familiaris	K254 (100%)			K675 (91%)	K734 (91%)	
Sus scrofa	K255 (100%)			K676 (91%)	K735 (91%)	
Homo sapiens	K260 (100%)	K264 (91%)		K653 (97%)	K728 (92%)	K786 (91%)

Table 7: Putative Lysines acetylation sites in NCX sequence in different species. Prediction was performed by using free software PHOSIDA.

The potential acetylation sites were further investigated in relation to their location in the protein structure and their potential functional impact. Structural models for the four conformational structural states of hSERCA2a (Figure 19) were generated with MODELLER (http://www.salilab.org/modeller/), based on rabbit homologue templates (83% sequence identity). On these different models, acetylated lysine sites were mapped on the hSERCA2a sequence and then their accessibility to acetylation and their location relative to functional sites were analyzed. Specifically, K464 and K585 were recognized as the best candidate acetylation sites, due to their location in the N-domain and being solvent accessible (Figure 19). Also K262 and K297 could be considered putative acetylated, but their location within the transmembrane domain suggested that they are not accessible for acetylation. Consequently, we decided to focus our attention only on K464 and K585.

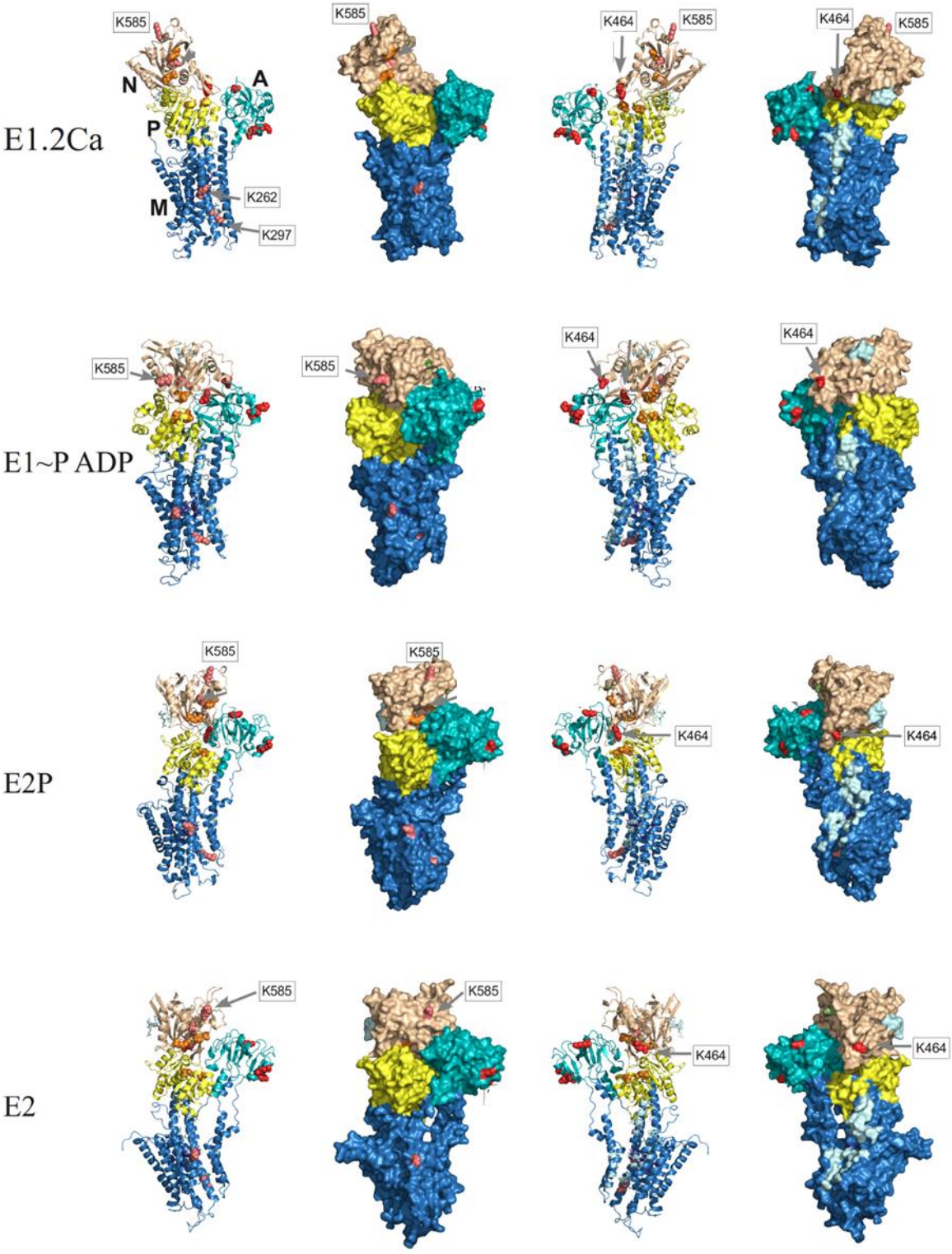
E1.2Ca
K585
N
A
P
M
K262
K297
K585
K464
K585
K464
K585
E1~P ADP
K585
K585
K464
K464
E2P
K585
K585
K464
K464
E2
K585
K585
K464
K464

Figure 19: Structural model of Serca2a in the four conformational states. Left column: cartoon representation. Second column: surface representation of the same orientation. Third and fourth columns: cartoon and surface representations of the model rotated 180° around vertical axis. The four domains (N,P,A and transmembrane domain M) are characterized by different colours (Legend is on the top left model). Acetylation sites are labelled, such as K464 and K585.

To evaluate the influence of Nε-lysine acetylation on hSERCA2 function, several mutants were produced where lysine in positions 464 or 585 was mutated into Glutamine (Q) or Arginine (R) to mimic constitutive acetylation or constitutive deacetylation, respectively. Transient transfection of vectors expressing either the hSERCA2 wild type form (WT) and the mutant forms was performed in HEK human cells, that express a lower levels of SERCA2 isoform compared to HL-1 cells and to other commonly used human cell line, such as HeLa (Figure 20).

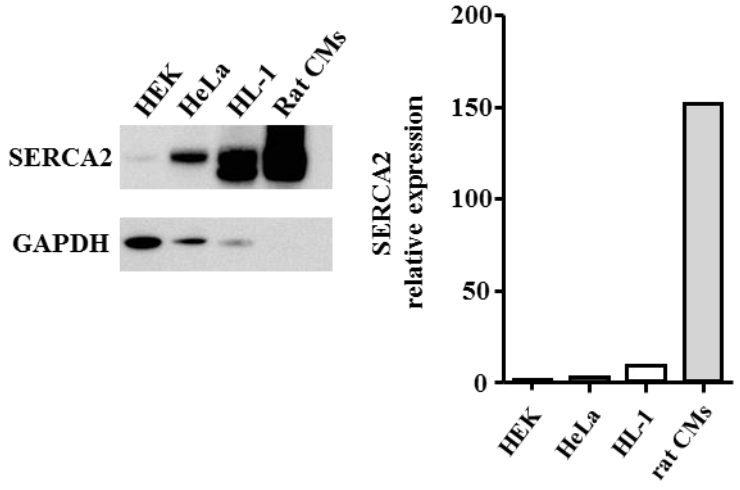

Figure 20: SERCA2 expression levels in different cells. Western blot analysis performed on HEK, HeLa, HL-1 cells and rat CMs. Densitometric analysis is on the right (n=1).

EFFECTS OF K464 AND K585 MUTATION ON HSERCA2 FUNCTION

Stably transfected HEK cells were loaded with the calcium sensitive dye Fluo-3 and after the application of a caffeine pulse, calcium transients were induced. The time of the recovery phase of Ca^{2+} transients was used to analyze SERCA2 function [13].

The time for the calcium traces to reach the fluorescence value equal to the 50% and the 90% of the baseline (time to BL 50% and time to BL 90%, respectively) was significantly postponed if compared to SERWT, when K464 was mutated into R (SERK464R) when compared to SERWT (Figure 21). Conversely, mutants where K464 was mutated into Q (SERK464Q) did not show any differences to the SERWT (Figure 21A, B). These results indicates that constitutive acetylation of hSERCA2 K464 does not induce an acceleration of the recovery phase of Ca^{2+} transient. Nevertheless, K464 mutation into R provokes a significant increase in the recovery phase time (Figure 21B), suggesting that the constitutive deacetylation has a negative impact on hSERCA2 function. Notably, mutations into Q and R of K585 did not induce any significant change in the time of recovery phase of Ca^{2+} transient (Figure 22A, B).

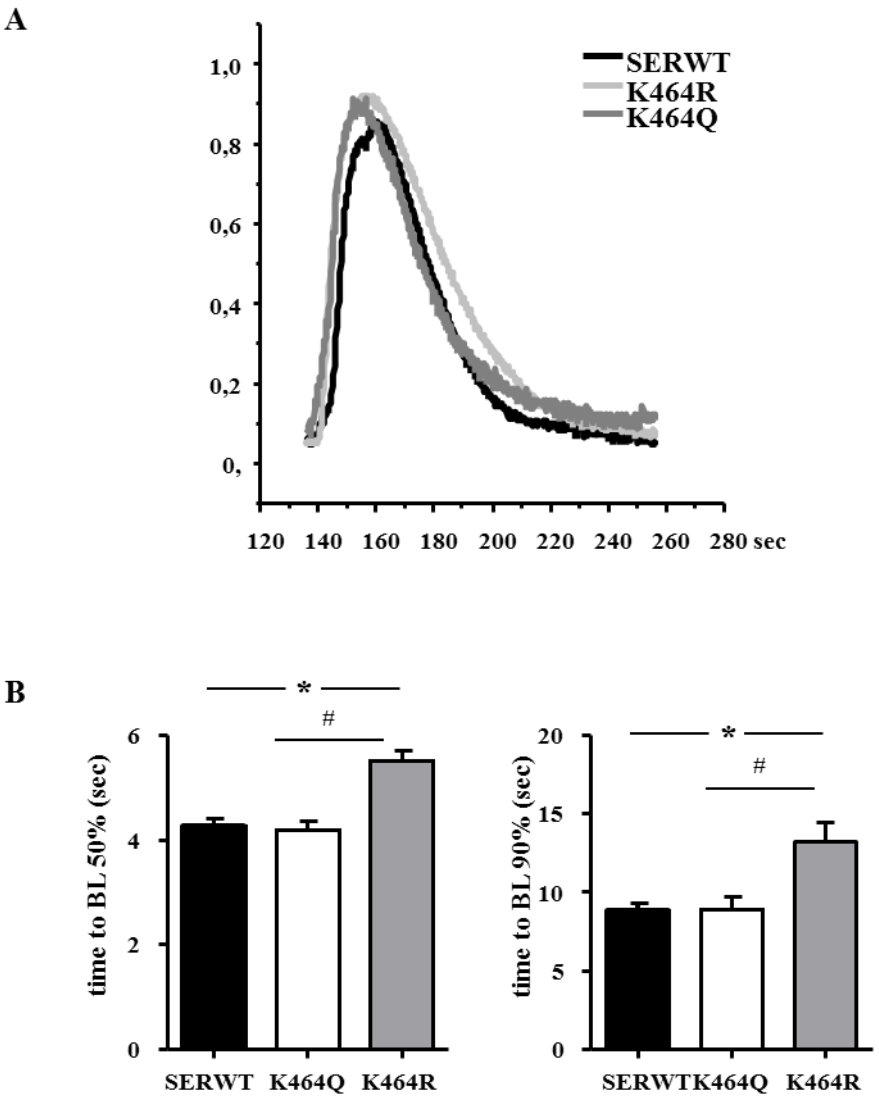

Figure 21: Changes in velocity of recovery of calcium transients in SERCA2 K464 mutants. K464 is mutated in Q or R. **(A)** Average of traces of calcium transients. **(B)** Calcium transients were evoked by caffeine pulse and then time to BL 50% and 90% were analyzed and represented in seconds (SERWT n =156, K464Q n = 62, K464R n = 34). Data are presented as mean ± sem, One-way ANOVA, followed by Bonferroni's multiple comparison correction, * $p < 0.05$ vs Ctrl; # $p < 0.05$ vs K464Q.

.

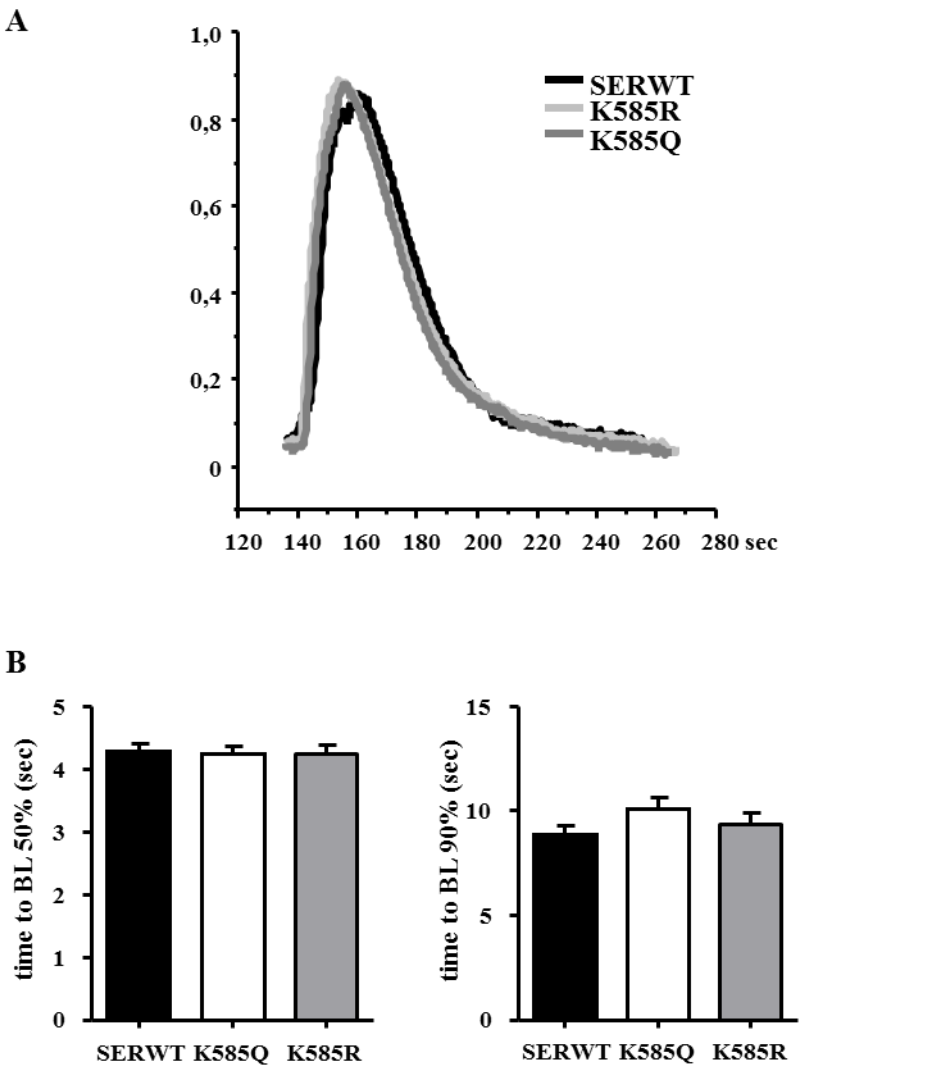

Figure 22: Changes in velocity of recovery of calcium transients in SERCA2 K585 mutants. K585 is mutated in Q or R. **(A)** Average of traces of calcium transients. **(B)** Calcium transients were evoked by caffeine pulse and then time to BL 50% and 90% were analyzed and represented in seconds (SERWT n =156, K585Q n = 76, K585R n = 57). Data are presented as mean ± sem, One-way ANOVA, followed by Bonferroni's multiple comparison correction.

DISCUSSION

SERCA2 activity has been proposed to be affected by acetylation/deacetylation processes by different authors [55; 59] even though, until now, no experimental confirmation has been described. In this work, we exhibited for the first time that SERCA2 direct acetylation can induce a significant increase of pump activity, as confirmed on isolated microsomes, and a consequent improvement of calcium removal parameters analyzed in different models of healthy and diseased cultured cardiomyocytes. Moreover, designated lysines have been modified in human SERCA2 protein in order to consider the role of specific acetylation sites.

In our experimental models, SERCA2 acetylation was induced by the treatment with Suberoylanilidehydroxamic acid (SAHA, or Vorinostat), an aspecific HDAC inhibitor. SAHA operates by chelating zinc ions in HDACs' active site and it acts on all class I and II HDACs at different concentrations [90, 76]. Notably, in October 2006 the US Food and Drug Administration (FDA) approved SAHA for the treatment of refractory cutaneous T-cell lymphoma [94]. Huber and coworkers [122] did *in vitro* studies on purified enzymes showing that class I HDAC isoforms 1, 2, and 8 are inhibited by SAHA (IC50 <20 nM). It is 100 fold less strong on HDAC3, while for the Class II HDAC, SAHA appears to be effective only at micromolar concentrations, inhibiting preferentially the mostly cytoplasmic isoform HDAC6. Several evidences have been provided in literature, presenting that SAHA stops cell growth of an extensive variety of transformed cells in culture at 0.5–10 μM [76, 93, 123, 124]. SAHA can act also on normal cells, but was establish to be selectively toxic to transformed cells, inducing death in tumor cells, although leaving normal cells viable and growth-inhibited [90]. The calculated 50% cytotoxic concentration (CC50) for different cell lines is described to be in the range of 7.5-14.1 μM [122]. In cellular assays with tumor cells, 2.5 μM is the reported optimal concentration for inducing differentiation [93]. The same concentration was used in different works where authors investigated SAHA effect on growth suppression and proliferation inhibition of tumoral cells [125, 126]. We applied the same concentration reported in literature for *in vitro* cellular studies but with a shorter treatment time, anyway comparable with the SAHA half-life in plasma [127]. HL-1 cells were treated with 2.5 μM of SAHA for 1.5 h and in these conditions, in agreement with literature data, we did not note cell cytotoxicity in term of vacuolarisation and/or mortality.

In HL-1 cardiomyocytes, the SERCA2 acetylation promoted by SAHA has been confirmed by immunoprecipitation and western blot for Acetil-Lysine. The specific SERCA2 ATPase activity has been investigated on isolated microsomes and resulted to be improved after HDAC inhibition. Specifically, at optimal calcium concentration (pCa5) [128, 129], we observed a statistically significant 2 fold increase of ATPase activity, demonstrating that SERCA2 acetylation promoted by SAHA induces an improvement of the enzyme activity, thus suggesting a faster reuptake of calcium into the SR. Moreover, we cannot exclude that SAHA can also act on other transporters or other proteins involved in calcium dynamic or on proteins that interact with SERCA2, but we have to take into consideration that SERCA2 is the most important player in calcium removal during the relaxation/recovery phase after the contraction. Actually, in different species (including humans, mice and rats) 70-90% of calcium ions are removed from the cytosol by SERCA2 [12]. Focusing our attention on the recovery phase of calcium transient, we investigated the effect of HDACs inhibition induced by SAHA in isolated zebrafish cardiomyocytes, as an alternative *ex-vivo* model. SERCA2 of zebrafish has an 88% sequence identity with the human protein sequence (data obtained by BLAST, http://blast.ncbi.nlm.nih.gov/Blast.cgi) and shares the same putative sites of acetylation (using PHOSIDA software). In zebrafish cardiomyocytes, parameters as time to baseline at 50 and 90% were significantly decreased after exposure to SAHA, confirming that, in this model, the recovery phase after the contraction is faster after SAHA treatment as suggested by the HL-1 model. Moreover, we performed measurements of NCX current in HL-1 cells not treated and treated with SAHA 2.5 μM to investigate the role of Sodium-Calcium exchanger and the possible effect of SAHA on this protein. Results showed that there were no changes in NCX current after SAHA adjunct, thus demonstrating that the observed effect of increased efficiency of calcium removal from cytoplasm was due only to SERCA2 activity. In conclusion, these data suggest that SERCA2 is modulated by the effect of HDAC inhibition.

We further study SAHA effect on rat cardiomyocytes. In rat cardiomyocytes we had to reduce the concentration of SAHA to 2.5 nM for a strong toxicity and mortality detected for higher concentrations. In any case, even at 2.5 nM there was an effect mediated by SAHA on the relaxation phase of cardiomyocytes contraction. In fact, also in this *ex-vivo* cellular model, an ameliorated time to re-lengthening was observed, thus

confirming that this phase, in which SERCA2 is the key player, is improved. Our findings are in accordance with previous data showing that the contractile activity of cardiomyocytes can be increased by the effect of HDACs inhibitors, enhancing calcium sensitivity of myofilaments [95].

In order to investigate the impact of SERCA2 increased acetylation in a pathological system, we study the effect of SAHA on cardiomyocytes isolated from a rat model of diabetes. It is widely recognized that diabetic cardiomyopathy may be characterized by early diastolic dysfunctions [17, 106, 130]. The most frequently used model of type 1 diabetes is streptozotocin (STZ) mode. STZ is a glucosamine-nitrosourea antibiotic that is analogous to glucose in term of structure [131] and it is usually given to animals to cause diabetes. Diabetes brings several modifications in STZ hearts: dysfunctions in Ca^{2+} handling, with a reduction in both activity and expression of SERCA2, a decrease in NCX expression, defects in sarcoplasmic reticulum calcium release and reuptake, and a compromised mitochondrial Ca^{2+} cycling [78, 132–136].
The reduction in SERCA2 activity and expression in the failing diabetic myocardium have been demonstrated as a main contributing feature of the diastolic dysfunction detected in heart failure [107]. Specifically, a minor SERCA2 expression decreases the Ca^{2+} taken into the SR and a decrease of SR Ca^{2+} level reduces the calcium available for the succeeding contraction–relaxation cycle [17].

We investigated the effect of HDACs inhibition on a STZ diabetic rat model, in order to consider if a restoration of normal values of SERCA2 activity could occur. As expected, after SAHA adjunct in diabetic rat cardiomyocytes both calcium transients and cell mechanical properties were improved, as well as SERCA2 activity measured in isolated microsomes, thus indicating that the dysfunction of calcium reuptake in diabetic cardiomyocytes can be restored by SAHA. Specifically, in diabetic rat cardiomyocytes the time required for cytosolic calcium re-uptake is prolonged, while the fraction of shortening is reduced. HDAC inhibition by SAHA treatment promoted a significant recovery of both parameters whose values approximated those measured in control cardiomyocytes.

In order to evaluate some conceivable acetylation sites able to influence SERCA2 activity, a bioinformatics prediction analysis has been done on the human SERCA2 sequence. The analysis has been performed modelling the human SERCA2 on the

published structure of rabbit SERCA1, based on rabbit homologue model (83% sequence identity). In relation to the accessibility by the solvent and the location within functional domains of the enzyme, the K464 was chosen as the highest scored lysine. Of note, this lysine has been described to be acetylated in guinea pig heart [59]. We created two mutants of human SERCA2, where K464 was mutated into Glutamine (Q) or Arginine (R) to mimic the acetylated and the deacetylated state of the residue, respectively. Exploring calcium transients in transfected HEK cells, an increase of the recovery time has been observed, when mimicking the deacetylated state of the K464, whereas no effect was detected when the acetylated state of K464 was reproduced. A possible reason could be that the K464 requires to be acetylated for protein normal activity. Further, due to its position near to the phospholamban binding site, it is also possible to hypothesize that acetylation at K464 could influence SERCA2 activity by changing the interaction between SERCA2 and PLB. However, it cannot be excluded that the increased activity of SERCA2 promoted by SAHA is the net effect of the acetylation at different sites at the same time.

In addition to the K464, we also made K585 mutants. This lysine could be theoretically acetylated as described in our prediction analysis, but Kho W. and coworkers reported that it can be SUMOylated [55]. In fact, SUMOylation of K585 enhances SERCA2a protein's stability and its calcium pump activity. SUMOylation is described to affect other PTMs in reciprocal and competitive ways, such as changing acetylation status [137]. In our experiments, no effects on recovery phase of calcium transients occurred after the mutations in K585, thus indicating that the acetylation is not the preferred post-translational modification on this site.

In summary, the results described in this study revealed that SERCA2 function can be modulated by pro-acetylating interventions. In fact, acetylation levels of the protein are increased after HDAC inhibition promoted by SAHA and its pump activity resulted to be improved in the different explored models, confirming that acetylation is a post-translational modification conserved among several species. Consequently, HAT/HDAC modulators can represent a starting point to develop drugs for the treatment of cardiac disorders where calcium handling is affected, such as diabetic cardiomyopathy, as already discussed in this work, but also heart failure or ventricular hypertrophy.

REFERENCES

[1] C. Toyoshima, "Structural aspects of ion pumping by Ca2+-ATPase of sarcoplasmic reticulum," *Arch. Biochem. Biophys.*, vol. 476, no. 1, pp. 3–11, 2008.

[2] L. Yatime, M. J. Buch-Pedersen, M. Musgaard, J. P. Morth, a. M. L. Winther, B. P. Pedersen, C. Olesen, J. P. Andersen, B. Vilsen, B. Schiøtt, M. G. Palmgren, J. V. Møller, P. Nissen, and N. Fedosova, "P-type ATPases as drug targets: Tools for medicine and science," *Biochim. Biophys. Acta - Bioenerg.*, vol. 1787, no. 4, pp. 207–220, 2009.

[3] M. Brini and E. Carafoli, "Calcium Pumps in Health and Disease," *Physiol Rev*, vol. 89, pp. 1341–1378, 2009.

[4] M. Periasamy and A. Kalyanasundaram, "SERCA pump isoforms: Their role in calcium transport and disease," *Muscle Nerve*, vol. 35, no. 4, pp. 430–442, 2007.

[5] E. Carafoli and M. Brini, "Calcium pumps: structural basis for and mechanism of calcium transmembrane transport," *Curr. Opin. Chem. Biol.*, vol. 4, no. 2, pp. 152–61, 2000.

[6] S. Dally, E. Corvazier, R. Bredoux, R. Bobe, and J. Enouf, "Multiple and diverse coexpression, location, and regulation of additional SERCA2 and SERCA3 isoforms in nonfailing and failing human heart," *J. Mol. Cell. Cardiol.*, vol. 48, no. 4, pp. 633–44, 2010.

[7] A.-M. Lompré, M. Anger, and D. Levitsky, "Sarco(endo)plasmic Reticulum calcium pumps in the cardiovascular system: function and gene expression," *J Mol Cell Cardiol*, vol. 26, pp. 1109–1121, 1994.

[8] a. L. Greene, M. J. Lalli, Y. Ji, G. J. Babu, I. Grupp, M. Sussman, and M. Periasamy, "Overexpression of SERCA2b in the heart leads to an increase in sarcoplasmic reticulum calcium transport function and increased cardiac contractility," *J. Biol. Chem.*, vol. 275, no. 32, pp. 24722–24727, 2000.

[9] P. Gélébart, V. Martin, J. Enouf, and B. Papp, "Identification of a new SERCA2 splice variant regulated during monocytic differentiation," *Biochem. Biophys. Res. Commun.*, vol. 303, no. 2, pp. 676–684, 2003.

[10] S. Dally, R. Bredoux, E. Corvazier, J. P. Andersen, J. D. Clausen, L. Dode, M. Fanchaouy, P. Gelebart, V. Monceau, F. Del Monte, J. K. Gwathmey, R. Hajjar, C. Chaabane, R. Bobe, A. Raies, and J. Enouf, "Ca2+-ATPases in non-failing and failing heart: evidence for a novel cardiac sarco/endoplasmic reticulum Ca2+-ATPase 2 isoform (SERCA2c).," *Biochem. J.*, vol. 395, no. 2, pp. 249–58, 2006.

[11] J. Dhitavat, R. J. Fairclough, a Hovnanian, and S. M. Burge, "Calcium pumps and keratinocytes : lessons from Darier ' s disease and Hailey – Hailey disease," *Br. J. Dermatol.*, vol. 150, pp. 821–828, 2004.

[12] D. M. Bers, “Calcium fluxes involved in control of cardiac myocyte contraction.,” *Circ. Res.*, vol. 87, no. 4, pp. 275–281, 2000.

[13] D. M. Bers, “Cardiac excitation–contraction coupling,” *Nature*, vol. 415, no. January, 2002.

[14] M. Arai, H. Matsui, and M. Periasamy, “Sarcoplasmic reticulum gene expression in cardiac hypertrophy and heart failure,” *Circ Res*, vol. 74, no. 4, pp. 555–564, 1994.

[15] V. Piacentino, “Cellular Basis of Abnormal Calcium Transients of Failing Human Ventricular Myocytes,” *Circ. Res.*, vol. 92, no. 6, pp. 651–658, 2003.

[16] M. Meyer, W. Schillinger, B. Pieske, C. Holubarsch, C. Heilmann, H. Posival, G. Kuwajima, K. Mikoshiba, H. Just, and G. Hasenfuss, “Alterations of Sarcoplasmic Reticulum Proteins in Failing Human Dilated Cardiomyopathy,” *Circulation*, vol. 92, no. 4, pp. 778–784, Aug. 1995.

[17] S. Boudina and E. D. Abel, “Diabetic Cardiomyopathy Revisited,” *Circulation*, vol. 115, no. 25, pp. 3213–3223, 2007.

[18] M. Sulaiman, M. J. Matta, N. R. Sunderesan, M. P. Gupta, M. Periasamy, and M. P. Gupta, “Resveratrol, an activator of SIRT1, upregulates sarcoplasmic calcium ATPase and improves cardiac function in diabetic cardiomyopathy.,” *Am. J. Physiol. Heart Circ. Physiol.*, vol. 298, no. 3, pp. H833–H843, 2010.

[19] M. D. Stern, “Theory of excitation-contraction coupling in cardiac muscle,” *Biophys. J.*, vol. 63, no. 2, pp. 497–517, 1992.

[20] D. Eisner, E. Bode, L. Venetucci, and A. Trafford, “Calcium flux balance in the heart.,” *J. Mol. Cell. Cardiol.*, vol. 58, pp. 110–7, 2013.

[21] R. A. Bassani, J. W. M. Bassani, and D. M. Bers, “Ralaxation in rabbit and rat cardiac cell: species-dependet differences in cellular mechanisms,” *J. Physiol.*, pp. 279–293, 1994.

[22] L. Hove-Madsen and D. M. Bers, “Sarcoplasmic reticulum Ca2+ uptake and thapsigargin sensitivity in permeabilized rabbit and rat ventricular myocytes.,” *Circ. Res.*, vol. 73, no. 5, pp. 820–828, 1993.

[23] L. Li, G. Chu, E. G. Kranias, and D. M. Bers, “Cardiac myocyte calcium transport in phospholamban knockout mouse: relaxation and endogenous CaMKII effects.,” *Am. J. Physiol.*, vol. 274, pp. H1335–H1347, 1998.

[24] G. Hasenfuss, “Animal models of human cardiovascular disease, heart failure and hypertrophy.,” *Cardiovasc. Res.*, vol. 39, no. 1, pp. 60–76, 1998.

[25] S. M. Pogwizd, K. Schlotthauer, L. Li, W. Yuan, and D. M. Bers, “Arrhythmogenesis and Contractile Dysfunction in Heart Failure,” *Circ. Res.*, vol. 88, pp. 1159–1167, 2001.

[26] C. Toyoshima, M. Nakasako, H. Nomura, and H. Ogawa, “Crystal structure of the calcium pump of sarcoplasmic reticulum at 2.6 A resolution,” *Nature*, vol. 405, no. M, pp. 647–655, 2000.

[27] C. Toyoshima and T. Mizutani, “Crystal structure of the calcium pump with a bound ATP analogue.,” *Nature*, vol. 430, no. 6999, pp. 529–535, 2004.

[28] C. Toyoshima, Y. Norimatsu, S. Iwasawa, T. Tsuda, and H. Ogawa, “How processing of aspartylphosphate is coupled to lumenal gating of the ion pathway in the calcium pump.,” *Proc. Natl. Acad. Sci. U. S. A.*, vol. 104, no. 50, pp. 19831–19836, 2007.

[29] C. Toyoshima, “How Ca2+-ATPase pumps ions across the sarcoplasmic reticulum membrane,” *Biochim. Biophys. Acta - Mol. Cell Res.*, vol. 1793, no. 6, pp. 941–946, 2009.

[30] C. Olesen, M. Picard, A.-M. M. L. Winther, C. Gyrup, J. P. Morth, C. Oxvig, J. V. Møller, P. Nissen, J. V Moller, and P. Nissen, “The structural basis of calcium transport by the calcium pump,” *Nature*, vol. 450, no. 7172, pp. 1036–1042, 2007.

[31] C. Toyoshima and H. Nomura, “Structural changes in the calcium pump accompanying the dissociation of calcium.,” *Nature*, vol. 418, no. 6898, pp. 605–611, 2002.

[32] C. Toyoshima and Inesi, “Structural basis of ion pumping by Ca2+ ATPase of the sarcoplasmic reticulum,” *Annu. Rev. Biochem.*, 2004.

[33] K. Obara, N. Miyashita, C. Xu, I. Toyoshima, Y. Sugita, G. Inesi, and C. Toyoshima, “Structural role of countertransport revealed in Ca(2+) pump crystal structure in the absence of Ca(2+).,” *Proc. Natl. Acad. Sci. U. S. A.*, vol. 102, no. 41, pp. 14489–14496, 2005.

[34] H. K. Simmerman and L. R. Jones, “Phospholamban: protein structure, mechanism of action, and role in cardiac function.,” *Physiol. Rev.*, vol. 78, no. 4, pp. 921–947, 1998.

[35] D. H. MacLennan and E. G. Kranias, “Phospholamban: a crucial regulator of cardiac contractility.,” *Nat. Rev. Mol. Cell Biol.*, vol. 4, no. 7, pp. 566–577, 2003.

[36] D. H. MacLennan, M. Abu-Abed, and C. Kang, “Structure–Function Relationships in Ca2+ Cycling Proteins,” *J. Mol. Cell. Cardiol.*, vol. 34, no. 8, pp. 897–918, 2002.

[37] P. Bhupathy, G. J. Babu, and M. Periasamy, “Sarcolipin and Phospholamban As Regulators of Cardiac Sarcoplasmic Reticulum Ca2+-ATPase,” *J Mol Cell Cardiol*, vol. 42, no. 5, pp. 903–911, 2007.

[38] A. Odermatt, P. E. Taschner, S. W. Scherer, B. Beatty, V. K. Khanna, D. R. Cornblath, V. Chaudhry, W. C. Yee, B. Schrank, G. Karpati, M. H. Breuning, N. Knoers, and D. H. MacLennan, “Characterization of the gene encoding human sarcolipin (SLN), a proteolipid associated with SERCA1: absence of structural mutations in five patients with Brody disease,” *Genomics*, vol. 45, no. 3, pp. 541–553, 1997.

[39] P. Vangheluwe, K. R. Sipido, L. Raeymaekers, and F. Wuytack, “New perspectives on the role of SERCA2’s Ca2+ affinity in cardiac function,” *Biochim. Biophys. Acta - Mol. Cell Res.*, vol. 1763, no. 11, pp. 1216–1228, 2006.

[40] A. Brittsan, “Phospholamban and Cardiac Contractile Function,” *J. Mol. Cell. Cardiol.*, vol. 32, no. 12, pp. 2131–2139, 2000.

[41] M. Tada, M. Kadoma, J. Fujii, Y. Kimura, and Y. Kijima, “Molecular structure and function of phospholamban: The regulatory protein of calcium pump in cardiac sarcoplasmic reticulum,” *Adv Exp Med Biol*, vol. 255, pp. 79–90, 1990.

[42] V. J. Kadambi and E. G. Kranias, “Phospholamban: a protein coming of age.,” *Biochem. Biophys. Res. Commun.*, vol. 239, no. 1, pp. 1–5, 1997.

[43] K. L. Koss and E. G. Kranias, “Phospholamban: A Prominent Regulator of Myocardial Contractility,” *Circ. Res.*, vol. 79, no. 6, pp. 1059–1063, Dec. 1996.

[44] A. Mattiazzi, C. Mundina- Weilenmann, C. Guoxiang, L. Vittone, and E. G. Kranias, “Role of phospholamban phosphorylation on Thr17 in cardiac physiological and pathological conditions,” *Cardiovasc. Res.*, vol. 68, no. 3, pp. 366–375, 2005.

[45] M. Periasamy, P. Bhupathy, and G. J. Babu, “Regulation of sarcoplasmic reticulum Ca2+ ATPase pump expression and its relevance to cardiac muscle physiology and pathology,” *Cardiovasc. Res.*, vol. 77, no. 2, pp. 265–273, 2008.

[46] M. Asahi, H. Nakayama, M. Tada, and K. Otsu, “Regulation of sarco(endo)plasmic reticulum Ca2+ adenosine triphosphatase by phospholamban and sarcolipin: implication for cardiac hypertrophy and failure.,” *Trends Cardiovasc. Med.*, vol. 13, no. 4, pp. 152–7, 2003.

[47] A. Odermatt, S. Becker, V. K. Khanna, K. Kurzydlowski, E. Leisner, D. Pette, and D. H. MacLennan, “Sarcolipin regulates the activity of SERCA1, the fast-twitch skeletal muscle sarcoplasmic reticulum Ca2+-ATPase.,” *J. Biol. Chem.*, vol. 273, no. 20, pp. 12360–12369, 1998.

[48] G. J. Babu, P. Bhupathy, C. A. Carnes, G. E. Billman, and M. Periasamy, “Differential expression of sarcolipin protein dring muscle development and cardiac pahtophysiology,” *J. Mol. Cell. Cardiol.*, vol. 43, no. 2, pp. 215–222, 2007.

[49] S. Minamisawa, “Atrial Chamber-specific Expression of Sarcolipin Is Regulated during Development and Hypertrophic Remodeling,” *J. Biol. Chem.*, vol. 278, no. 11, pp. 9570–9575, 2003.

[50] P. Vangheluwe, S. M, Z. E, W. E, R. L, and W. F, “Sarcolipin and phospholamban mRNA and protein expression in cardiac and skeletal muscle of different species,” *Biochem. J.*, vol. 159, pp. 151–159, 2005.

[51] D. H. MacLennan, A. M, and T. A. Russel, “The regulation of SERCA-type pumps by phospholamban and sarcolipin,” *Ann. N.Y. Acad. Sci*, pp. 472–480, 2003.

[52] G. J. Babu, P. Bhupathy, N. N. Petrashevskaya, H. Wang, S. Raman, D. Wheeler, G. Jagatheesan, D. Wieczorek, A. Schwartz, P. M. L. Janssen, M. T. Ziolo, and M. Periasamy, “Targeted Overexpression of Sarcolipin in the Mouse Heart Decreases Sarcoplasmic Reticulum Calcium Transport and Cardiac Contractility,” *J. Biol. Chem.*, vol. 281, no. 7, pp. 3972–3979, 2006.

[53] I. Vandecaetsbeek, P. Vangheluwe, L. Raeymaekers, F. Wuytack, and J. Vanoevelen, “The Ca2+ Pumps of the Endoplasmic Reticulum and Golgi Apparatus,” *Cold Spring Harb. Perspect Biol*, 2011.

[54] A. N. Stammers, S. E. Susser, N. C. Hamm, M. W. Hlynsky, D. E. Kimber, D. S. Kehler, and T. A. Duhamel, “The regulation of sarco(endo)plasmic reticulum calcium-ATPases (SERCA)1,” *Can. J. Physiol. Pharmacol.*, 2015.

[55] C. Kho, A. Lee, D. Jeong, J. G. Oh, A. H. Chaanine, E. Kizana, W. J. Park, and R. J. Hajjar, “SUMO1-dependent modulation of SERCA2a in heart failure,” *Nature*, vol. 477, no. 7366, pp. 601–605, 2012.

[56] T. Adachi, R. M. Weisbrod, D. R. Pimentel, J. Ying, V. S. Sharov, C. Schöneich, and R. A. Cohen, “S-Glutathiolation by peroxynitrite activates SERCA during arterial relaxation by nitric oxide.,” *Nat. Med.*, vol. 10, no. 11, pp. 1200–7, 2004.

[57] K. R. Bidasee, Y. Zhang, C. H. Shao, M. Wang, K. P. Patel, Ü. D. Dincer, and H. R. Besch, “Diabetes Increases Formation of Advanced Glycation End Products on Sarco(endo)plasmic Reticulum Ca2+-ATPase,” *Diabetes*, vol. 53, no. 2, pp. 463–473, 2004.

[58] T. V Knyushko, V. S. Sharov, T. D. Williams, C. Schöneich, and D. J. Bigelow, “3-Nitrotyrosine modification of SERCA2a in the aging heart: a distinct signature of the cellular redox environment.,” *Biochemistry*, vol. 44, no. 39, pp. 13071–81, 2005.

[59] D. B. Foster, T. Liu, J. Rucker, R. N. O’Meally, L. R. Devine, R. N. Cole, and B. O’Rourke, “The cardiac acetyl-lysine proteome.,” *PLoS One*, vol. 8, no. 7, p. e67513, 2013.

[60] T. Kouzarides and T. Kouzarides, “NEW EMBO MEMBER’S REVIEW Acetylation: a regulatory modi cation to rival phosphorylation?,” *EMBO J.*, vol. 19, no. 6, pp. 1176–1179, 2000.

[61] X. J. Yang, “Lysine acetylation and the bromodomain: A new partnership for signaling,” *BioEssays*, vol. 26, pp. 1076–1087, 2004.

[62] K. K. Lee and J. L. Workman, “Histone acetyltransferase complexes: one size doesn’t fit all,” *Nat. Rev. Mol. Cell Biol.*, vol. 8, no. 4, pp. 284–295, 2007.

[63] M. D. Shahbazian and M. Grunstein, “Functions of site-specific histone acetylation and deacetylation.,” *Annu. Rev. Biochem.*, vol. 76, pp. 75–100, 2007.

[64] K. Sadoul, C. Boyault, M. Pabion, and S. Khochbin, “Regulation of protein turnover by acetyltransferases and deacetylases,” *Biochimie*, vol. 90, no. 2, pp. 306–312, 2008.

[65] C. Choudhary, C. Kumar, F. Gnad, M. L. Nielsen, M. Rehman, T. C. Walther, J. V Olsen, and M. Mann, “Lysine acetylation targets protein complexes and co-regulates major cellular functions.,” *Science*, vol. 325, no. 5942, pp. 834–840, 2009.

[66] M. A. Glozak, N. Sengupta, X. Zhang, and E. Seto, “Acetylation and deacetylation of non-histone proteins.,” *Gene*, vol. 363, pp. 15–23, 2005.

[67] A. Riccio, “Dynamic epigenetic regulation in neurons: enzymes, stimuli and signaling pathways.,” *Nat. Neurosci.*, vol. 13, no. 11, pp. 1330–1337, 2010.

[68] A. J. Bannister and T. Kouzarides, “Regulation of chromatin by histone modifications,” *Cell Res.*, vol. 21, no. 3, pp. 381–395, 2011.

[69] S. Y. Roth, J. M. Denu, and D. Allis, “Histone Acetyltransferases,” *Annu. Rev. Biochem*, vol. 70, pp. 81–120, 2001.

[70] D. E. Sterner and S. L. Berger, “Acetylation of histones and transcription-related factors,” *Microbiol. Mol. Biol. Rev.*, vol. 64, no. 2, pp. 435–459, 2000.

[71] R. H. Goodman and S. Smolik, “CBP / p300 in cell growth , transformation , and development,” *Genes Dev.*, vol. 14, no. 1997, pp. 1553–1577, 2000.

[72] Y. Xue-Franzén, A. Johnsson, D. Brodin, J. Henriksson, T. R. Bürglin, and A. P. H. Wright, “Genome-wide characterisation of the Gcn5 histone acetyltransferase in budding yeast during stress adaptation reveals evolutionarily conserved and diverged roles.,” *BMC Genomics*, vol. 11, p. 200, 2010.

[73] C. Simone, S. V. Forcales, D. a Hill, A. N. Imbalzano, L. Latella, and P. L. Puri, “p38 pathway targets SWI-SNF chromatin-remodeling complex to muscle-specific loci,” *Nat. Genet.*, vol. 36, no. 7, pp. 738–743, 2004.

[74] Y. Gao, C. C. Hubbert, and T. Yao, “The Microtubule-associated Histone Deacetylase 6 (HDAC6) Regulates Epidermal Growth Factor Receptor (EGFR) Endocytic Trafficking and Degradation,” *J. Biol. Chem.*, vol. 285, no. 15, pp. 11219–11226, 2010.

[75] J. E. Bolden, M. J. Peart, and R. W. Johnstone, “Anticancer activities of histone deacetylase inhibitors,” *Nat. Rev. Drug Discov.*, vol. 5, no. 9, pp. 769–784, 2006.

[76] P. Marks, R. A. Rifkind, V. M. Richon, R. Breslow, T. Miller, and W. K. Kelly, “Histone deacetylases and cancer: causes and therapies.,” *Nat. Rev. Cancer*, vol. 1, no. 3, pp. 194–202, 2001.

[77] M. Dokmanovic, C. Clarke, and P. A. Marks, “Histone Deacetylase Inhibitors: Overview and Perspectives,” *Mol. Cancer Res.*, vol. 5, no. 10, pp. 981–989, 2007.

[78] K. Zhao, R. Harshaw, X. Chai, and R. Marmorstein, “Structural basis for nicotinamide cleavage and ADP-ribose transfer by NAD(+)-dependent Sir2 histone/protein deacetylases.,” *Proc. Natl. Acad. Sci. U. S. A.*, vol. 101, no. 23, pp. 8563–8568, 2004.

[79] A. A. Sauve, C. Wolberger, V. L. Schramm, and J. D. Boeke, “The Biochemistry of Sirtuins,” *Annu. Rev. Biochem.*, vol. 75, no. 1, pp. 435–465, 2006.

[80] A. J. M. de Ruijter, A. H. van Gennip, H. N. Caron, S. Kemp, and A. B. P. van Kuilenburg, “Histone deacetylases (HDACs): characterization of the classical HDAC family.,” *Biochem. J.*, vol. 370, no. Pt 3, pp. 737–49, 2003.

[81] M. S. Longworth and L. a Laimins, “Histone deacetylase 3 localizes to the plasma membrane and is a substrate of Src.,” *Oncogene*, vol. 25, no. 32, pp.

4495–500, 2006.

[82] P. a Marks and R. Breslow, “Dimethyl sulfoxide to vorinostat: development of this histone deacetylase inhibitor as an anticancer drug.,” *Nat. Biotechnol.*, vol. 25, no. 1, pp. 84–90, 2007.

[83] M. Dokmanovic and P. A. Marks, “Prospects: Histone deacetylase inhibitors,” *J. Cell. Biochem.*, vol. 96, no. 2, pp. 293–304, 2005.

[84] S. Minucci and P. G. Pelicci, “Histone deacetylase inhibitors and the promise of epigenetic (and more) treatments for cancer,” *Nat. Rev. Cancer*, vol. 6, no. 1, pp. 38–51, 2006.

[85] C. Dinarello and G. Fossati, “Histone Deacetylase Inhibitors for Treating a Spectrum of Diseases Not Related to Cancer,” *Mol. Med.*, vol. 17, no. 5–6, p. 1, 2011.

[86] B. R. Selvi, J.-C. C. Cassel, T. K. Kundu, and A.-L. L. Boutillier, “Tuning acetylation levels with HAT activators: therapeutic strategy in neurodegenerative diseases.,” *Biochim. Biophys. Acta*, vol. 1799, no. 10–12, pp. 840–853, 2010.

[87] Mwakwari SC, P. V, G. W, and O. AK, “Macrocyclic Histone Deacetylase Inhibitors,” *Curr Top Med Chem*, vol. 18, no. 9, pp. 1199–1216, 2010.

[88] T. Miller, D. Witter, and S. Belvedere, “Histone deacetylase inhibitors,” *J. Med. Chem.*, vol. 46, no. 24, pp. 1–13, 2003.

[89] N. Batty, G. G. Malouf, and J. P. J. Issa, “Histone deacetylase inhibitors as anti-neoplastic agents,” *Cancer Lett.*, vol. 280, no. 2, pp. 192–200, 2009.

[90] V. M. Richon, “Cancer biology: mechanism of antitumour action of vorinostat (suberoylanilide hydroxamic acid), a novel histone deacetylase inhibitor,” *Br. J. Cancer*, vol. 95, pp. S2–S6, 2006.

[91] M. Yoshidas, M. Yoshida, M. Kijima, M. Akita, and T. Beppu, “Potent and specific inhibition of mammalian histone deacetylase both in vivo and in vitro by trichostatin A.,” *J. Biol. Chem.*, vol. 265, no. 28, pp. 17174–17179, 1990.

[92] S. Belvedere, D. J. Witter, J. Yan, J. P. Secrist, V. Richon, and T. a Miller, “Aminosuberoyl hydroxamic acids (ASHAs): a potent new class of HDAC inhibitors.,” *Bioorg Med Chem lett*, vol. 17, no. 14, pp. 3969–71, 2007.

[93] V. M. Richon, S. Emiliani, E. Verdin, Y. Webb, R. Breslow, R. a Rifkind, and P. A. Marks, “A class of hybrid polar inducers of transformed cell differentiation inhibits histone deacetylases.,” *Proc. Natl. Acad. Sci. U. S. A.*, vol. 95, no. 6, pp. 3003–7, 1998.

[94] B. S. Mann, J. R. Johnson, M. H. Cohen, R. Justice, and R. Pazdur, “FDA approval summary: vorinostat for treatment of advanced primary cutaneous T-cell lymphoma.,” *Oncologist*, vol. 12, no. 10, pp. 1247–52, 2007.

[95] M. P. Gupta, S. A. Samant, S. H. Smith, and S. G. Shroff, “HDAC4 and PCAF Bind to Cardiac Sarcomeres and Play a Role in Regulating Myofilament Contractile Activity,” *J. Biol. Chem.*, vol. 283, no. 15, pp. 10135–10146, 2008.

[96] C. Colussi, R. Berni, J. Rosati, S. Straino, S. Vitale, F. Spallotta, S. Baruffi, L. Bocchi, F. Delucchi, S. Rossi, M. Savi, D. Rotili, F. Quaini, E. MacChi, D. Stilli, E. Musso, A. Mai, C. Gaetano, and M. C. Capogrossi, "The histone deacetylase inhibitor suberoylanilide hydroxamic acid reduces cardiac arrhythmias in dystrophic mice," *Cardiovasc. Res.*, vol. 87, no. 1, pp. 73–82, 2010.

[97] Y.-H. Kao, J.-P. Liou, C.-C. Chung, G.-S. Lien, C.-C. Kuo, S.-A. Chen, and Y.-J. Chen, "Histone deacetylase inhibition improved cardiac functions with direct antifibrotic activity in heart failure.," *Int. J. Cardiol.*, vol. 168, no. 4, pp. 4178–83, Oct. 2013.

[98] W. C. Claycomb, N. a Lanson, B. S. Stallworth, D. B. Egeland, J. B. Delcarpio, A. Bahinski, and N. J. Izzo, "HL-1 cells: a cardiac muscle cell line that contracts and retains phenotypic characteristics of the adult cardiomyocyte," *Proc. Natl. Acad. Sci. U. S. A.*, vol. 95, no. 6, pp. 2979–2984, 1998.

[99] D. D. Belke and W. H. Dillmann, "Altered cardiac calcium handling in diabetes.," *Curr. Hypertens. Rep.*, vol. 6, no. 6, pp. 424–9, 2004.

[100] L. J. Field, "Atrial natriuretic factor-SV40 T antigen transgenes produce tumors and cardiac arrhythmias in mice," *Science*, vol. 239, no. 4843, p. 1029—1033, Feb. 1988.

[101] S. M. White, P. E. Constantin, and W. C. Claycomb, "Cardiac physiology at the cellular level: use of cultured HL-1 cardiomyocytes for studies of cardiac muscle cell structure and function," *Am. J. Physiol. Heart Circ. Physiol.*, vol. 286, no. 3, pp. H823–H829, 2004.

[102] K. Kitta, S. a Clément, J. Remeika, J. B. Blumberg, and Y. J. Suzuki, "Endothelin-1 induces phosphorylation of GATA-4 transcription factor in the HL-1 atrial-muscle cell line.," *Biochem. J.*, vol. 359, no. Pt 2, pp. 375–80, 2001.

[103] L. Sartiani, P. Bochet, E. Cerbai, A. Mugelli, and R. Fischmeister, "Functional expression of the hyperpolarization-activated, non-selective cation current I_f in immortalized HL-1 cardiomyocytes," *J. Physiol.*, vol. 545, no. 1, pp. 81–92, 2002.

[104] G. JC, M. CL, and L. RT, "Regenerative biology," *Cold Spring Harb. Perspect Med*, 2013.

[105] W. E. Louch, K. A. Sheehan, and B. M. Wolska, "Methods in Cardiomyocyte Isolation, Culture, and Gene Transfer," *J Mol Cell Cardiol.*, vol. 51, no. 3, pp. 288–298, 2011.

[106] K. Wei, T. Eckmanns, M. Oppert, M. Martin, R. Amorosa, I. Zuschneid, U. Frei, H. Ru, and M. I. Care, "The Streptozotocin-Diabetic Chronic Complications Rat as a Model of the of Human Diabetes," *Hear. Lung Circ.*, 2003.

[107] A. Zarain-Herzberg, G. García-Rivas, and R. Estrada-Avilés, "Regulation of SERCA pumps expression in diabetes.," *Cell Calcium*, vol. 56, no. 5, pp. 1–9, 2014.

[108] P. Nemtsas, E. Wettwer, T. Christ, G. Weidinger, and U. Ravens, "Adult zebrafish heart as a model for human heart? An electrophysiological study.," *J.*

Mol. Cell. Cardiol., vol. 48, no. 1, pp. 161–71, 2010.

[109] A. K. Robbins and A. Horlick, "Macrophage Scavenger Receptor Confers an Adherent Phenotype to Cells in Culture," *Biotechniques*, vol. 25, pp. 240–244, 1998.

[110] C. Colussi, J. Rosati, S. Straino, F. Spallotta, R. Berni, D. Stilli, S. Rossi, E. Musso, E. Macchi, A. Mai, G. Sbardella, S. Castellano, C. Chimenti, A. Frustaci, A. Nebbioso, L. Altucci, M. C. Capogrossi, and C. Gaetano, "Nε-lysine acetylation determines dissociation from GAP junctions and lateralization of connexin 43 in normal and dystrophic heart.," *Proc. Natl. Acad. Sci. U. S. A.*, vol. 108, no. 18, pp. 2795–2800, 2011.

[111] C. L. Andersen, J. L. Jensen, and T. F. Ørntoft, "Normalization of real-time quantitative reverse transcription-PCR data: a model-based variance estimation approach to identify genes suited for normalization, applied to bladder and colon cancer data sets.," *Cancer Res.*, vol. 64, no. 15, pp. 5245–5250, 2004.

[112] K. J. Livak and T. D. Schmittgen, "Analysis of relative gene expression data using real-time quantitative PCR and the 2-ÄÄCT method.," *Methods*, vol. 25, no. 4, pp. 402–408, 2001.

[113] K. E. I. Maruyama and D. H. MacLennan, "Mutation of aspartic acid-351, lysine-352, and lysine-515 alters the Ca2+ transport activity of the Ca2+-ATPase expressed in COS-1 cells," *Proc. Natl. Acad. Sci. U. S. A.*, vol. 85, no. May, pp. 3314–3318, 1988.

[114] F. Gnad, J. Gunawardena, and M. Mann, "PHOSIDA 2011: the posttranslational modification database," *Nucleic Acids Res.*, vol. 39, no. Database, pp. D253–D260, 2011.

[115] M. F. Chou and D. Schwartz, "Biological Sequence Motif Discovery Using motif-x," *Curr Protoc Bioinforma.*, vol. Chapter 13, no. September, p. Unit 13.15–24, 2011.

[116] D. Schwartz, M. F. Chou, and G. M. Church, "Predicting Protein Post-translational Modifications Using Meta-analysis of Proteome Scale Data Sets," *Mol. Cell. Proteomics*, vol. 8, no. 2, pp. 365–379, 2009.

[117] B. Webb and A. Sali, "Comparative Protein Structure Modeling Using MODELLER.," *Curr Protoc Bioinforma.*, vol. 47, pp. 5.6.1–5.6.32, Jan. 2014.

[118] M. A. Martí-Renom, A. C. Stuart, S. Roberto, F. Melo, and S. Andrej, "Comparative protein structure modeling of genes and genomes," *Annu. Rev. Biophys. Biomol.Struct.*, pp. 291–325, 2000.

[119] V. Parente, S. Balasso, G. Pompilio, L. Verduci, G. I. Colombo, G. Milano, U. Guerrini, L. Squadroni, F. Cotelli, O. Pozzoli, and M. C. Capogrossi, "Hypoxia/Reoxygenation Cardiac Injury and Regeneration in Zebrafish Adult Heart," *PLoS One*, vol. 8, no. 1, p. e53748, 2013.

[120] C. Jopling, E. Sleep, M. Raya, M. Martí, A. Raya, and C. I. Belmonte, "Zebrafish heart regeneration occurs by cardiomyocyte dedifferentiation and proliferation," *Nature*, vol. 464, no. 7288, pp. 606–609, 2010.

[121] M. Zaniboni, a E. Pollard, L. Yang, and K. W. Spitzer, "Beat-to-beat repolarization variability in ventricular myocytes and its suppression by electrical coupling," *Am. J. Physiol. Heart Circ. Physiol.*, vol. 278, no. 3, pp. H677–H687, 2000.

[122] K. Huber, J. Plaks, E. Fyne, J. W. Mellors, and N. Sluis-cremer, "Inhibitors of Histone Deacetylases - Correlation between isoform specificity and reactivation of HIV type 1 (HIV-1) from latently infected cells," *J. Biol. Chem.*, vol. 286, no. 25, pp. 22211–22218, 2011.

[123] P. A. Marks and M. Dokmanovic, "Histone deacetylase inhibitors: discovery and development as anticancer agents," *Expert Opin. Investig. Drugs*, Nov. 2005.

[124] C.-Y. Gui, L. Ngo, W. S. Xu, V. M. Richon, and P. a Marks, "Histone deacetylase (HDAC) inhibitor activation of p21WAF1 involves changes in promoter-associated proteins, including HDAC1.," *Proc. Natl. Acad. Sci. U. S. A.*, vol. 101, no. 5, pp. 1241–1246, 2004.

[125] V. M. Richon, T. W. Sandhoff, R. a Rifkind, and P. a Marks, "Histone deacetylase inhibitor selectively induces p21WAF1 expression and gene-associated histone acetylation.," *Proc. Natl. Acad. Sci. U. S. A.*, vol. 97, no. 18, pp. 10014–10019, 2000.

[126] L. M. Butler, X. Zhou, W.-S. Xu, H. I. Scher, R. A. Rifkind, P. A. Marks, and V. M. Richon, "The histone deacetylase inhibitor SAHA arrests cancer cell growth, up-regulates thioredoxin-binding protein-2, and down-regulates thioredoxin.," *Proc. Natl. Acad. Sci. U. S. A.*, vol. 99, no. 18, pp. 11700–5, 2002.

[127] R. a Parise, J. L. Holleran, J. H. Beumer, S. Ramalingam, and M. J. Egorin, "A liquid chromatography-electrospray ionization tandem mass spectrometric assay for quantitation of the histone deacetylase inhibitor, vorinostat (suberoylanilide hydroxamicacid, SAHA), and its metabolites in human serum.," *J. Chromatogr. B. Analyt. Technol. Biomed. Life Sci.*, vol. 840, no. 2, pp. 108–15, 2006.

[128] Lytton, Westlin, Burk, Shull, and MacLennan, "Functional Comparisions between Isoforms of the Sarcoplasmic of Endoplasmic Reticulum Family of Calcium Pumps," *J. Biol. Chem.*, vol. 267, pp. 14483–14489, 1992.

[129] Q. Yao, L. T. L. Chen, J. Li, K. Brungardt, T. C. Squier, and D. J. Bigelow, "Oligomeric Interactions between Phospholamban Molecules Regulate Ca-ATPase Activity in Functionally Reconstituted Membranes †," *Biochemistry*, vol. 40, no. 21, pp. 6406–6413, 2001.

[130] I. I. Joffe, K. E. Travers, C. L. Perreault-micale, T. Hampton, S. E. Katz, J. P. Morgan, and P. S. Douglas, "Abnormal Cardiac Function in the Non – Insulin-Dependent Diabetic Rat," *J. Am. Coll. Cardiol.*, vol. 34, no. 7, pp. 2111–9, 1999.

[131] W. J. Schnedl, S. Ferber, J. H. Johnson, and C. B. Newgard, "STZ transport and cytotoxicity: Specific enhancement in GLUT2-expressing cells," *Diabetes*, vol. 43, no. 11, pp. 1326–1333, 1994.

[132] G. D. Lopaschuk, A. G. Tahiliani, R. V. Vadlamudi, S. Katz, and J. H. McNeill, "Cardiac sarcoplasmic reticulum function in insulin- or carnitine-treated diabetic

rats," *Am J Physiol Hear. Circ Physiol*, vol. 245, no. 6, pp. H969–976, Dec. 1983.

[133] C. E. Flarsheim, I. L. Grupp, and M. A. Matlib, "Mitochondrial dysfunction accompanies diastolic dysfunction in diabetic rat heart," *Am J Physiol Hear. Circ Physiol*, vol. 271, no. 1, pp. H192–202, Jul. 1996.

[134] Y. Hattori, N. Matsuda, J. Kimura, T. Ishitani, A. Tamada, S. Gando, O. Kemmotsu, and M. Kanno, "Diminished function and expression of the cardiac Na+-Ca2+ exchanger in diabetic rats: implication in Ca2+ overload.," *J. Physiol.*, vol. 527 Pt 1, pp. 85–94, 2000.

[135] K. M. Choi, Y. Zhong, B. D. Hoit, I. L. Grupp, H. Hahn, K. W. Dilly, S. Guatimosim, W. J. Lederer, and M. A. Matlib, "Defective intracellular Ca(2+) signaling contributes to cardiomyopathy in Type 1 diabetic rats," *Am J Physiol Hear. Circ Physiol*, vol. 283, no. 4, pp. H1398–408, 2002.

[136] W. L. Suarez-Pinzon, R. F. Power, H. Yan, C. Wasserfall, M. Atkinson, and A. Rabinovitch, "Combination therapy with glucagon-like peptide-1 and gastrin restores normoglycemia in diabetic NOD mice," *Diabetes*, vol. 57, no. 12, pp. 3281–3288, 2008.

[137] C. Van Rechem, G. Boulay, S. Pinte, N. Stankovic-Valentin, C. Guérardel, and D. Leprince, "Differential regulation of HIC1 target genes by CtBP and NuRD, via an acetylation/SUMOylation switch, in quiescent versus proliferating cells,"

APPENDIX

Acetylation is correlated to aging and to different diseases such as cancer, retroviral pathogenesis, neurodegenerative and cardiovascular diseases. Several protein properties can be regulated by lysine acetylation, including DNA-protein interaction, transcriptional activity, subcellular localization, stability and contribution in signaling pathways. It has been reported that, at the chromatin level, gene expression can be regulated by the balance between acetylation and deacetylation of both histone and non-histone proteins. In fact, HATs and HDACs are enzymes that can alter the chromatin condensation status, thus allowing it to have a significant role in transcription [1].

Furthermore, several evidences reported that exposure to electric activity have an impact on different cell functions: cell migration [2], development [3], wound healing, nerve growth, angiogenesis [4] and metastases [5] can be modulated by electric signals and transcription of excitable cells is influenced by electrical activity.

Epigenetic modifications of DNA and histone proteins are emerging as important mechanisms by which cells adapt their transcriptional response to developmental and environmental signals. For example, mechanisms by which extracellular signals regulate the activity of chromatin-modifying enzymes has been reported in the nervous system, where depolarization allows the activation of the HAT CBP (chromatin binding protein, p300) promoting an increase of intracellular Ca^{2+} concentration through the activation of L-type Ca^{2+} channels [6, 7]. In the context of cardiac function, cell pacing can promote the transcriptional regulation of genes such as GATA4, Adss1 (adenylosuccinate synthetase 1 [8]) and STAT3. Further, high frequency electrical stimulation can induce the hypertrophic growth of cultured cardiomyocytes [9], [10]. Notably, altered expression and/or localization of Connexin43 (Cx43) is reported in cardiac rhythm diseases, as atrial fibrillation (AF) and tachycardia-associated remodeling [11]. Connexin43 is the major component of gap junctions (GJs) connecting cardiomyocytes [12]. However, mechanisms of how electrical stimulation may affect Cx43 expression, function and distribution in diseases associated with rhythm disorders is not completely clear.

It has been recently shown that tachypacing can cause electrical remodeling and cardiomyocytes loss of function , partially due to HDAC6 activation and consequent deacetylation-induced depolymerization of α-tubulin [13]. Moreover, it has been demonstrated that HDAC4 and PCAF play a role in the regulation of cardiac

myofilament contraction in an acetylation-dependent manner [14]. In addition, lysine acetylation can modify Cx43 expression and its intracellular distribution, thus influencing cell to cell communication with consequences on cardiac function [15].

The following appendix would offer an overview on electrical activity and its impact on cell acetylation and, consequently, cardiac function.

During the three years of my PhD in Systemic Pathophysiology, I focus my attention on drug-induced and activity-dependent acetylation as a new perception of the regulation of cardiac function. The thesis that I presented investigate the role of acetylation in the modulation of cardiac cell activity, specifically the impact of SERCA2 acetylation (promoted by HDAC inhibition after SAHA treatment) on its calcium pumping activity. On the other side it was of interest analyzing whether the cardiac cell activity could be modulated by acetylation of cardiac proteins. To attend this, I gave my contribute in the work titled "Acetylation mediates Cx43 reduction caused by electrical stimulation", under the supervision of Dr. Alessandra Rossini.

This project took in consideration the alteration of electrical activity and its regulation of communication between cardiomyocytes by influencing the acetylation status of Cx43. Specifically, it provides evidences that the junctional remodeling consequent to altered electrical activity can be partially explained by variation in acetylation/deacetylation balance of cardiomyocytes. Electrical stimulation can modulate Cx43 acetylation in cardiac cells both *in vivo* and *in vitro* with a consequent down-regulation and intracellular relocalization of Cx43. This work suggests that electrical activity-dependent alteration of protein acetylation might be a novel mechanism for the regulation of cardiomyocyte communication and support the hypothesis that HAT/HDAC modulators could play a role in new approaches for rhythm disturbance regulation.

The work has been published in the Journal of Molecular and Cellular Cardiology, Volume 87, October 2015, Pages 54–64 (doi:10.1016/j.yjmcc.2015.08.001).

REFERENCES

[1] Z. Wang, C. Zang, K. Cui, D. E. Schones, A. Barski, W. Peng, and K. Zhao, "Genome-wide Mapping of HATs and HDACs Reveals Distinct Functions in Active and Inactive Genes.," *Cell*, vol. 138, no. 5, pp. 1019–1031, 2009.

[2] A. Guo, B. Song, B. Reid, Y. Gu, J. V Forrester, C. a B. Jahoda, M. Zhao, and et al., "Effects of Physiological Electric Fields on Migration of Human Dermal Fibroblasts," *J Invest Dermatol*, vol. 130, no. 9, pp. 2320–2327, 2010.

[3] C. D. McCaig and M. Zhao, "Physiological electrical fields modify cell behaviour.," *Bioessays*, vol. 19, no. 9, pp. 819–26, Sep. 1997.

[4] B. Song, M. Zhao, J. V Forrester, and C. D. McCaig, "Nerve regeneration and wound healing are stimulated and directed by an endogenous electrical field in vivo," *J. Cell Sci.*, vol. 117, no. 20, pp. 4681–4690, 2004.

[5] K. R. Robinson and M. A. Messerli, "Left/right, up/down: the role of endogenous electrical fields as directional signals in development, repair and invasion.," *Bioessays*, vol. 25, no. 8, pp. 759–66, Aug. 2003.

[6] A. Riccio, "Dynamic epigenetic regulation in neurons: enzymes, stimuli and signaling pathways.," *Nat. Neurosci.*, vol. 13, no. 11, pp. 1330–1337, 2010.

[7] G. E. Hardingham, S. Chawla, F. H. Cruzalegui, and H. Bading, "Control of Recruitment and Transcription-Activating Function of CBP Determines Gene Regulation by NMDA Receptors and L-Type Calcium Channels," *Neuron*, vol. 22, no. 4, pp. 789–798, 1999.

[8] Y. Xia, J. B. McMillin, A. Lewis, M. Moore, W. G. Zhu, R. S. Williams, and R. E. Kellems, "Electrical stimulation of neonatal cardiac myocytes activates the NFAT3 and GATA4 pathways and up-regulates the adenylosuccinate synthetase 1 gene," *J. Biol. Chem.*, vol. 275, no. 3, pp. 1855–1863, 2000.

[9] McDonough and Glembotski, "Induction of Atrial Natriuretic Factor and Myosin Light Chain-2 gene expression in cultured ventricular Myocytes by electrical stimulation of contraction," *J. Biol. Chem.*, pp. 11665–11668, 1992.

[10] C. T. Ivester, R. L. Kent, H. Tagawa, H. Tsutsui, T. Imamura, G. . 4th Cooper,

and P. J. McDermott, “Electrically stimulated contraction accelerates protein synthesis rates in adult feline cardiocytes,” *Am J Physiol Hear. Circ Physiol*, vol. 265, no. 2, pp. H666–674, Aug. 1993.

[11] F. Molica, M. J. P. Meens, S. Morel, and B. R. Kwak, “Mutations in cardiovascular connexin genes.,” *Biol. Cell*, vol. 106, no. 9, pp. 269–93, Sep. 2014.

[12] X. Lin, J. Gemel, A. Glass, C. W. Zemlin, E. C. Beyer, and R. D. Veenstra, “Connexin40 and connexin43 determine gating properties of atrial gap junction channels,” *J. Mol. Cell. Cardiol.*, vol. 48, no. 1, pp. 238–245, 2010.

[13] D. Zhang, C.-T. Wu, X. Qi, R. A. M. Meijering, F. Hoogstra-Berends, A. Tadevosyan, G. Cubukcuoglu Deniz, S. Durdu, A. R. Akar, O. C. M. Sibon, S. Nattel, R. H. Henning, and B. J. J. M. Brundel, “Activation of Histone Deacetylase-6 Induces Contractile Dysfunction Through Derailment of α-Tubulin Proteostasis in Experimental and Human Atrial Fibrillation,” *Circulation*, vol. 129, no. 3, pp. 346–358, 2014.

[14] M. P. Gupta, S. A. Samant, S. H. Smith, and S. G. Shroff, “HDAC4 and PCAF Bind to Cardiac Sarcomeres and Play a Role in Regulating Myofilament Contractile Activity,” *J. Biol. Chem.*, vol. 283, no. 15, pp. 10135–10146, 2008.

[15] C. Colussi, J. Rosati, S. Straino, F. Spallotta, R. Berni, D. Stilli, S. Rossi, E. Musso, E. Macchi, A. Mai, G. Sbardella, S. Castellano, C. Chimenti, A. Frustaci, A. Nebbioso, L. Altucci, M. C. Capogrossi, and C. Gaetano, “Nε-lysine acetylation determines dissociation from GAP junctions and lateralization of connexin 43 in normal and dystrophic heart.,” *Proc. Natl. Acad. Sci. U. S. A.*, vol. 108, no. 18, pp. 2795–2800, 2011.

LIST OF FULL LENGTH PUBLICATIONS

Acetylation mediates Cx43 reduction caused by electrical stimulation
V. Meraviglia, V. Azzimato, C. Colussi, **M.C. Florio**, A. Binda, A. Panariti, K. Qanud, S.Suffredini, L. Gennaccaro, M. Miragoli, A. Barbuti, P. D. Lampe, C. Gaetano, P. P. Pramstaller, M. C. Capogrossi, F. A. Recchia, G. Pompilio, I. Rivolta, A. Rossini
Journal of Molecular and Cellular Cardiology - J Mol Cell Cardiol. 2015 Oct; 87:54-64

Higher cardiogenic potential of IPSCs derived from cardiac versus skin stromal cells
V. Meraviglia, J. Wen, L. Piacentini, G. Campostrini, C. Wang, **M.C. Florio**, V. Azzimato, L. Fassina, M. Langes, J. Wong, M. Miragoli, C. Gaetano, G. Pompilio, A. Barbuti, D. DiFrancesco, D. Mascalzoni, P. P. Pramstaller, G. I. Colombo, H. S. V. Chen, A. Rossini
Frontiers in Bioscience, Landmark, 21, 719-743, January 1, 2016